



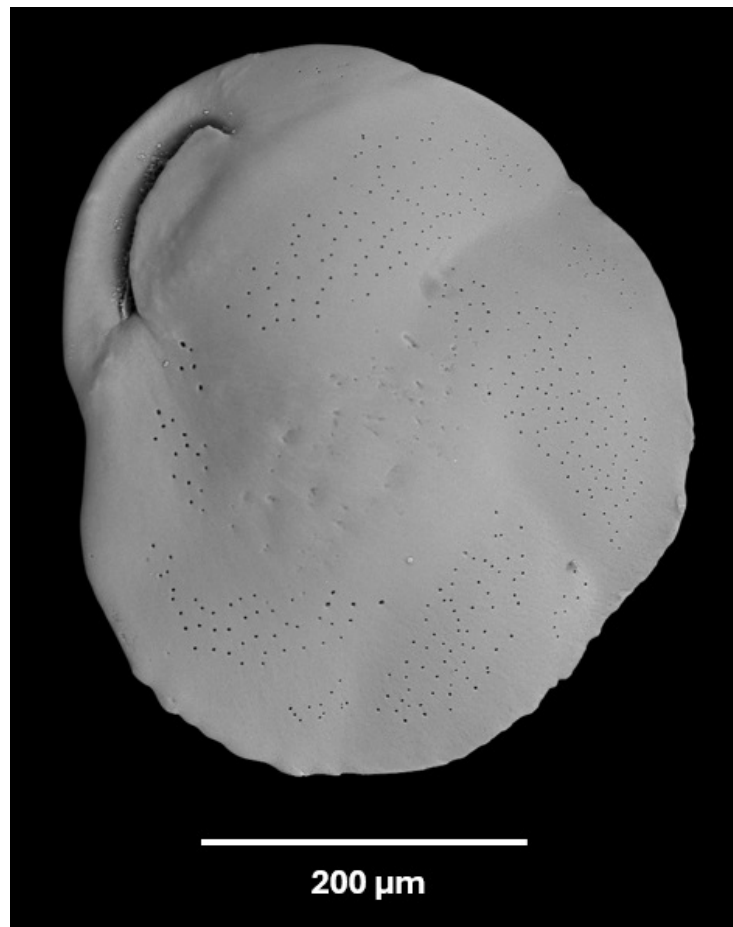
Stockholm
University

Bachelor Thesis

Degree Project in
Earth Science 30 hp

Testing the utility of *Cassidulina neoteretis* for biostratigraphic dating in Arctic Ocean sediments

Anke Fries



Stockholm 2024

Department of Geological Sciences
Stockholm University
SE-106 91 Stockholm

Testing the utility of *Cassidulina neoteretis* for biostratigraphic dating in Arctic Ocean sediments

Abstract

The low diversity and abundance of living organisms and their fossil remains makes biostratigraphic dating in Arctic sediments particularly challenging. The benthic foraminifera *Cassidulina neoteretis* is a common species in the Arctic environment today and differs slightly in morphology from its ancestor *Cassidulina teretis*, making the evolutionary transition between the two species a potential biostratigraphic age marker. In this study, 1031 specimens from six cores from different Arctic regions were imaged and compared to test the utility of this event. The apertural flap that is smooth in *C. neoteretis* and serrated in *C. teretis* was proposed to be a valuable characteristic for identification, which could be confirmed in this project. Novelty, evidence is brought forth that pore size could also be an important indicator to differentiate both species. In two cores from the Southern Lomonosov Ridge the *C. neoteretis/teretis* transition, including the loss of serration and increase in pore size, could be pinpointed to depths of 171 cm to 183 cm (LOMROG07PC04) and 127 cm to 142 cm (LOMROG12PC03). It coincides with other changes in benthic foraminiferal assemblages, showing that the *C. neoteretis/teretis* transition could not only be an important marker event, but also be indicative of global cooling and variations in sea ice cover.

Contents

1. Introduction	4
1.1 Background	4
1.2 Site details	7
1.3 Other relevant benthic foraminifera species	8
1.4 Aim and research questions	10
2. Material and methods	11
2.1 Material	11
2.2 Light microscope and SEM imaging.....	12
2.2 Morphometrics	13
3. Results	14
3.1 Key characteristics of <i>Cassidulina neoteretis</i> and <i>teretis</i>	14
3.2 Changes through time in core LOMROG07PC04	20
3.3 Morphological variability.....	24
3.4 Comparison with core LOMROG12PC03	26
3.5 Observations from other regions	27
4. Discussion	29
4.1 From <i>teretis</i> to <i>neoteretis</i>	29
4.2 Signs of a cooling climate	30
4.3 Meaning of apertural change	32
4.4 Age models and tentative dating of the <i>C. neoteretis/teretis</i> transition.....	33
4.5 Evaluation of the utility	36
4.6 Critical reflection	37
4.7 Future research opportunities	38
5. Conclusion	39
6. Acknowledgements	39
References	39
Appendix A SEM images	44
Appendix B data tables	52

Introduction

1.1 Background

The Arctic Ocean is one of the least studied oceans of our planet, mostly because of its inaccessibility. Especially dating of Arctic sediments is challenging, as the extreme polar environment limits the application of traditional methods such as magnetostratigraphy, oxygen isotope chemostratigraphy or biostratigraphy. In this project, the utility of a potential biostratigraphic marker, the evolutionary transition between the two foraminiferal species *Cassidulina teretis* and *Cassidulina neoteretis*, is analysed.

Foraminifera are marine single-celled organisms (protozoans), that possess a hard, agglutinated or calcareous shell (Haynes, 1981). Soft, shell-less foraminifera have been observed as well, but as they leave no fossil record, they are less useful for paleontological reconstructions. The size of foraminifera is generally below 1 mm, but some can exceed a few cm (Murray, 2006, BouDagher-Fadel, 2008). There are planktonic foraminifera living in the upper water column and benthic foraminifera living on the seafloor. As protection for their inner cell body, foraminifera secrete a calcareous shell, also known as their test (Fig. 1), which can also sometimes be formed by cementing grains of sediments together. The test is generally constructed by incremental additions, new interconnected chambers that are being added in times of abundant food supply (Loeblich and Tappan, 1988). For respiration, attachment or movement, feeding, building of new shell and reproduction, benthic foraminifera use pseudopodia (Haynes, 1981), which are extending from the aperture, the “mouth” of a specimen (Fig.1&2). The pseudopodia are made of organic material and not preserved in the fossil record. Most foraminifera can move via self-locomotion, but more efficiently travel with ocean currents or attached to sediment grains, boats, and animals (Murray, 2006); this way they might be able to disperse over distances up to 3000 km (Patterson et al., 1997).

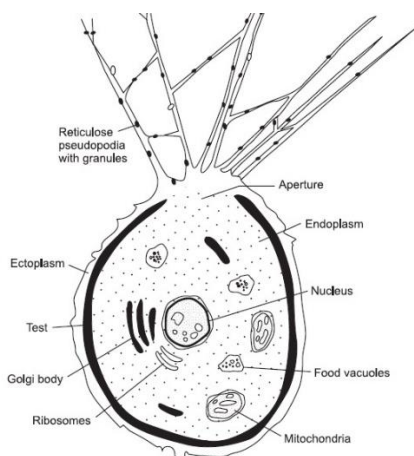


Fig.1: Benthic foraminiferid in cross-section (Armstrong and Brasier, 2005).



Fig.2: Light microscope image showing the morphology of *Cassidulina neoteretis*. Coloured outlines identify test features relevant for identification. Scalebar = 200 µm

The importance of foraminifera for the bio-geosciences lies in their abundance and globality as well as their outstanding preservation as fossils. There are over 10.000, possibly up to 15.000, extant species of foraminifera (Ald et al., 2007) and between 100 and 10.000 living foraminifera individual specimens over 63 μm can be found per 100 cm^2 surface area in marine sediments (Murray, 2006). Some taxa can even live in transitional brackish environments, including lagoons and estuaries (du Châtelet et al., 2018). They respond quickly to their surroundings, making them useful indicators of environmental change (Schönfeld et al., 2012). Through different analyses, fossil foraminifera can be used to reconstruct paleoclimates and -environments. For example, Mg/Ca-ratios of their tests can be analysed to reconstruct ocean temperatures. Oxygen and carbon isotopes can indicate salinity and ocean circulation and allow reconstructions of former sea levels and global sea ice volume (Gooday & Jorissen, 2012). Nowadays, because of their quick adaptation to changes, benthic foraminifera are also commonly used to monitor the anthropogenic impact on the marine ecosystem (Gooday & Jorissen, 2012). What makes them of utter utility for science is that in some cases their age can be determined. Often, foraminiferal assemblages and their stratigraphic range are so well-preserved that they allow the dating of sediment layers, which otherwise, especially in extreme environments, can be a challenging task. It is therefore of utmost importance that the distinct species that can be indicative of specific time frames and environments are properly identified.

Foraminifera have evolutionary adapted throughout Earth's history and, depending on their habitat, different species have developed various morphological features to fill distinct ecological niches. The key factors influencing the development of benthic foraminiferal species brought forward by Murray (2006) are salinity, temperature, concentration of dissolved oxygen, abundance of food and nutrients, properties of the seafloor, competition, and space. Because of the large varieties, a multitude of studies were executed that describe benthic foraminifera around the globe and in the most diverse environments (e.g., Giraldo-Gomez et al., 2022 in the central-Pacific; Majewski et al., 2023, in sub-Antarctic fjords; or Bulian et al., 2022 in the Mediterranean). This project is focusing solely on the Arctic habitat, as Arctic sediments are in desperate need of reliable age markers. Dating in the Arctic is difficult because of low sedimentation rates, and hostile living conditions that lead to low biological diversity. Another difficulty arises from the issue that uniform palaeomagnetic reversal patterns in the Arctic Ocean do not correlate to the global geomagnetic polarity timescale (GPTS), otherwise one of the most useful tools for relative dating (Alexandersson et al., 2014). Calcareous nannofossils, that elsewhere are routinely used for biostratigraphy, are scarce in Quaternary Arctic sediments but can prove very useful (Razmjooei et al., 2023). A reliable biostratigraphic age marker from the world of foraminifera could be a real asset for dating in the Arctic.

Even though foraminifera show large variability, some species can look remarkably similar, only distinguished by rather small morphological features, but nonetheless have different ecologies. The persistent taxonomic confusion between morphologically similar taxa is still a widespread problem in benthic foraminifera research (Cage et al., 2021). In the Arctic this is especially the case for two very alike species: *Cassidulina neoteretis* and *Cassidulina teretis*. *C. neoteretis*

presumably evolved from *C. teretis* between 2.0 and 2.3 million years ago in the North Atlantic and from then migrated northwards (Seidenkrantz, 1995), where it is now primarily found in cool, stable Arctic and subarctic subsurface waters (Cage et al., 2021). *C. neoteretis* is present throughout the central Arctic Ocean and is the most common species at water depths of 500 m to 1100 m (Osterman et al., 1999). The first occurrence of *C. teretis* was in the Middle Miocene and it is considered to be extinct since the Pleistocene. In its time it extended into shallower and possibly warmer habitats, thereby having a wider ecological range than *C. neoteretis* (Seidenkrantz, 1995). The study of Seidenkrantz (1995) was based in the North Atlantic, so further evidence is necessary to confirm if the same applies to the central Arctic. The characteristic features shared by *C. neoteretis* and *C. teretis* are a lenticular shape of the calcareous test, an elongated aperture, a prominent often milky umbilical boss, eight to ten biserially arranged chambers and a flattened peripheral keel (Fig.2). The biggest morphological differences between the two species according to Seidenkrantz (1995) are the shape of the apertural flap and whether or not there is a fringe of small serrations or teeth (Fig. 3) and the generally smaller size of *C. neoteretis*.

Since the last well-documented occurrence of *C. teretis* was 0.7 million years ago (Ma) (Seidenkrantz, 1995), being able to clearly distinguish it from *C. neoteretis* can help to give a very quick estimation of the age of sediment layers and their paleoenvironment; if the clear distinction can be made, it might even be established as a biostratigraphical marker. Currently, this is however poorly established in the Arctic. A previous study in the western Arctic Ocean from Lazar et al., 2016 concluded that the *C. neoteretis/teretis* transition was not a reliable evolutionary event and rather time transgressive. No such study has been conducted in the Eurasian Arctic. More evidence from different Arctic regions is necessary to better understand the evolution and distribution of *C. neoteretis* and *C. teretis*. The main focus of this thesis is on those two species, because they are very common in Arctic sediments and could prove useful for biostratigraphy and reconstructions of the paleoclimate. Nonetheless, other similar species as *Cassidulina laevigata* and *Cassidulina reniforme* will also be described and outlined, because it is crucial to avoid any source of confusion.

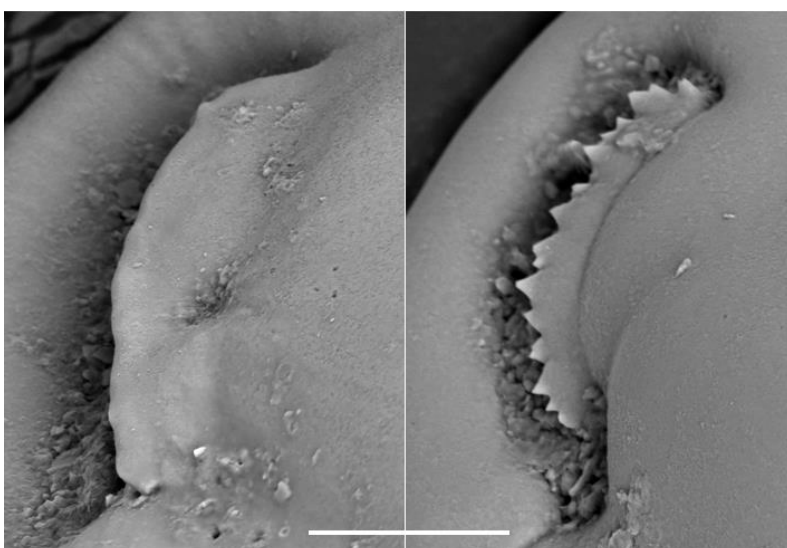


Fig.3: Scanning electron microscope images showing the apertural flap of *Cassidulina neoteretis* from LOMROG07PC04, 2-3 cm depth (left) and *Cassidulina teretis* from LOMROG07PC04, 300-301 cm depth (right). The right picture clearly shows the typical prominent teeth of *C. teretis*. Scalebar = 30 μ m

1.2 Site details

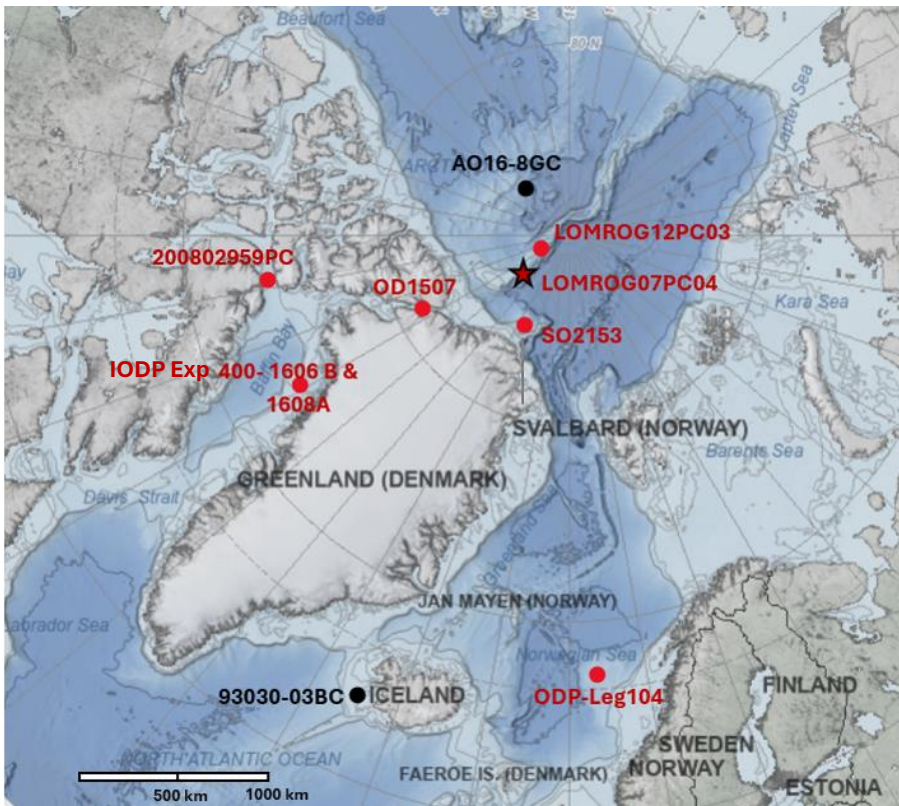


Fig.4: Overview of the core sites from which the researched samples originated, marked in red are samples in which *C. neoteretis* and/or *C. teretis* were captured. The star marks the LOMROG07PC04 site, which delivered most data for this study with its extraordinary abundance of benthic foraminifera.

Credit: NOAA National Environmental Satellite, Data, and Information Service (NESDIS), National Centers for Environmental Information (NCEI); International Bathymetric Chart of the Arctic Ocean (IBCAO); General Bathymetric Chart of the Oceans (GEBCO); Natural Earth.

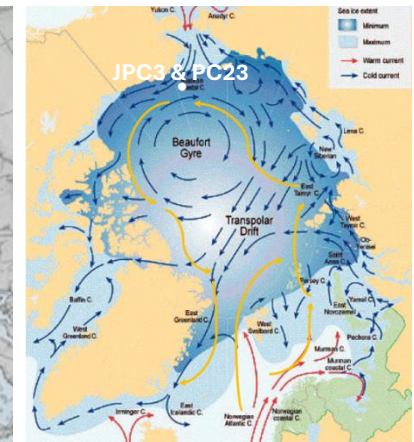


Fig.5: Arctic Ocean circulation. Blue arrows indicate cold surface currents, red arrows warm surface currents and orange arrows intermediate Atlantic water. Marked in white are the core sites researched by Lazar et al., 2016. Modified from Tremblay et al., 2005.

Ten sites in various geographical regions of the Arctic Ocean (Fig.4) and from different water depths (Table 1) have been chosen to give a generous picture of the variety in morphologies of *C. neoteretis*. All data were gathered from elevated ridges and plateaus because they have higher sedimentation rates, less pronounced calcite dissolution and no influence of turbidites (Backman et al., 2004) and therefore a higher probability of containing calcareous foraminifera. Whereas AO16-8GC is under the influence of the Beaufort Gyre, the other sites are affected by the Transpolar Drift or North Atlantic surface currents (Fig.5). Even though these are surface currents, they are highly important for benthic foraminifera, as their food intake relies heavily on surface water conditions. At intermediate depths, warm, saline North Atlantic water enters the Arctic and circulates counterclockwise along the shelf margins (Farmer et al., 2010). As *C. neoteretis* probably migrated from the North Atlantic and is generally associated with intermediate Atlantic water (Cage et al., 2021), this Arctic intermediate water (AIW) could also

be an important factor in the development of *C. neoteretis* in the Arctic Ocean. Baffin Bay receives influx of both Atlantic and Pacific water, making it an interesting study site.

Sample site	Location	Longitude	Latitude	water depth
200802959PC	Lancaster Sound	74°25.9623	-82°38.415	791 m
93030-03BC	Southwestern Iceland Shelf	64°18.00	-24°13.90	250 m
AO168GC	Alpha Ridge	86°77.95	-14°06.433	2620 m
IODPEXP4001606B	Baffin Bay	74°14.28	-61°1.6553	656 m
IODPEXP4001608A	Baffin Bay	74°7.6818	-60°58.3172	607 m
LOMROG07PC04	Southern Lomonosov Ridge	86°42.07	-53°46.03	810 m
LOMROG12PC03	Southern Lomonosov Ridge	87°43.29	-54°25.31	1607 m
OD1507	Petermann Fjord	80°73.73	-60°78.45	570 m
ODPLeg104	Norwegian Sea	67°13.5	02°055.7	1286 m
SO2153Bx11	Morris Jessup Rise	84°31.204	-24°31.712	1364 m

Table 1: Overview of the geographical distribution of the core sites and their water depths.

Except for the two southmost sites 93030-03BC and ODP-Leg104, all core sites lie under a sea ice cover for most of the year, making research challenging and data scarce, especially during the winter.

1.3 Other relevant benthic foraminifera species

The persistent taxonomic confusion between morphological similar taxa is a frequent problem in the studies of benthic foraminifera (Cage et al., 2021). This often leads to different species being grouped together which might result in a flawed interpretation of fossil assemblages. Osterman (1996) for example noted that *C. teretis* was difficult to distinguish from *Islandiella helenae* and *Islandiella norcrossi* and grouped them all into one *C. teretis* category. To avoid any potential sources of confusion, as a first step, the relevant species shall be named, imaged, and described. Cage et al. (2021) gave a good overview on how the *Cassidulina* group can be clearly distinguished from *Islandiella* and *Paracassidulina* by looking at the shape of the aperture (Fig.6). *Cassidulina* has a narrow slit with an apertural plate, *Paracassidulina*'s apertural slit is much longer and has a narrow edge, and *Islandiella* has a broader triangular to elliptical opening on the margin of the final chamber from which a free apertural tongue is protruding (Cage et al., 2021). The colour of *Islandiella* tends to be of a “colder” white, whereas *Cassidulina* exhibits a “warmer” white, and the umbilical boss of *Islandiella* tends to be transparent whereas *Cassidulina* is more likely to have a milky umbilical boss (Cage et al., 2021). The latter readily visually observable differences also depend on the state of preservation and regional varieties and cannot serve as a singular characteristic for identification. Based on the paper of Cage et al. (2021) it was possible within the frame of this project to identify and differentiate the *Cassidulina* group from the *Paracassidulina* and *Islandiella* group and the latter two shall therefore not be investigated any further. All similar species within the *Cassidulina* group, *Cassidulina obtusa*, *Cassidulina laevigata*, *Cassidulina reniforme*, *Cassidulina cf. reniforme* as well as *Cassidulina neoteretis* and *Cassidulina teretis* are described in detail in the results.

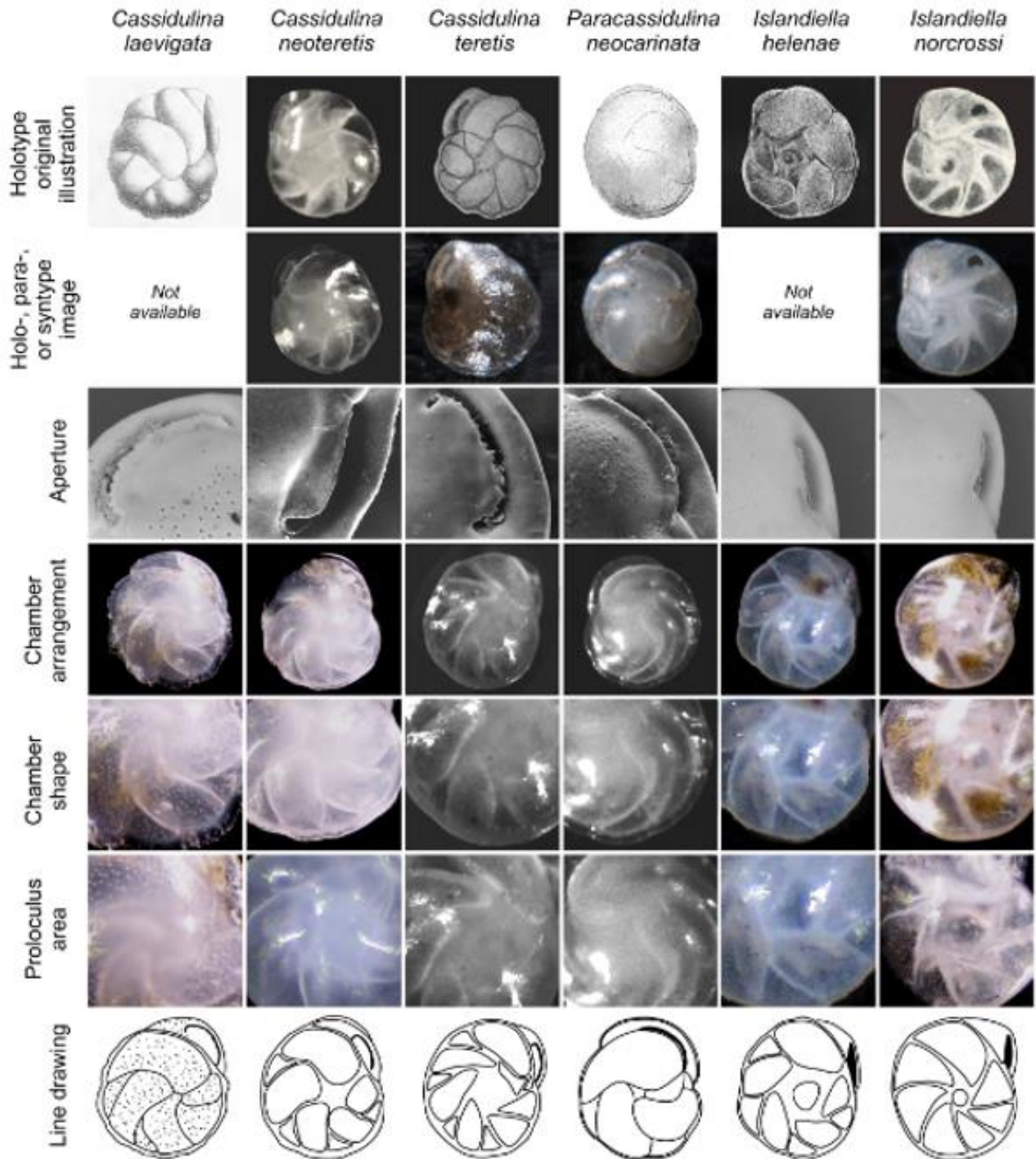


Fig.6: Comparison of the characteristic morphological features of *Cassidulina laevigata*, *Cassidulina neoteretis*, *Cassidulina teretis*, *Paracassidulina neocarinata*, *Islandiella helenae* and *Islandiella norcrossi*. Taken from Cage et al. (2021). This classification framework was central for taxonomic identification of foraminifera in this study.

1.4 Aim and research questions

The aim of this project is to clear up confusion on frequent taxonomic issues and provide additional data for the Arctic Ocean, where tangible information is rare and valid age models are often wishful thinking. It also attempts to shine a light on the world of *Cassidulina*, which has a myriad of possible research opportunities.

The distinction between *C. neoteretis* and *C. teretis* in the literature is not always consistent, often possibly because scientists are not even aware that there is a difference. Scott et al. (2008) for one labelled apertural features as not useful for telling the two species apart because of their variability and grouped all specimens into *C. teretis*, including what prior workers had assigned to *C. teretis* and/or *C. neoteretis* (Cronin et al., 2019). Especially older studies often only mention *C. teretis* (e.g. Wollenburg and Mackensen, 1998), whereas recent studies might only refer to *C. neoteretis* (e.g. Hanslik, PhD thesis, 2011) often having no conclusive description or images of the specimens, making it impossible to know which species was encountered. The first step is therefore to investigate how the two species can be identified and differentiated. Seidenkrantz (1995) states that the apertural flaps of *C. neoteretis* are always much smoother than in *C. teretis*, which typically has teeth, and that the average diameter of *C. neoteretis* ranges between 260 µm and 300 µm, whereas *C. teretis* has a much larger range between 250 µm and 550 µm. It needs to be confirmed by more data if these features can really be used as a general characteristic distinction. This leads to the postulation of the first research question:

- (I) Can *C. neoteretis* and *C. teretis* in the Eurasian Arctic and Baffin Bay reliably be distinguished by their morphology, especially by the shape of their apertural flaps and their size, but also by porosity or direction of coiling?

According to Seidenkrantz (1995) *C. neoteretis* presumably evolved from *C. teretis* in the North Atlantic between about 2.0 and 2.3 Ma. As the last well-documented appearance of *C. teretis* and the first occurrence of *C. neoteretis* in the Norwegian Sea happened just above the paleomagnetic Brunhes/Matuyama boundary around 0.7 Ma, the transition could prove to be a valuable biostratigraphic marker. Cage et al. (2021) bring forward that in most studies of temporal intervals all specimens will belong to either *C. teretis* or *C. neoteretis* and the differentiation could be used to assign sediments to Pliocene or possibly older Pleistocene (*C. teretis*) or late Quaternary and Holocene (*C. neoteretis*). In 2016, Lazar et al. reevaluated the utility of *C. neoteretis* as a biostratigraphic marker and found no clear stratigraphic pattern of change in the western Arctic. After finding *C. neoteretis* only in the youngest sediments (upper 10 cm), the authors are suggesting that they are rather ecophenotypes than different species. This leads to the postulation of the second research question:

- (II) Is the transition from *C. teretis* to *C. neoteretis* evident in different Arctic regions and could it be used as a biostratigraphic marker event?

Material and methods

2.1 Material

The study sites were chosen based on their location to give the best possible overview on the whole situation in the Arctic Ocean, and on availability, for example no samples from the western Arctic were obtainable. Cores were chosen from localities that are influenced by different surface currents: The Amerasian Basin under control of the Beaufort Gyre (AO16-8GC), the Eurasian Basin (SO2153) and the Norwegian Sea (ODPLeg104) largely influenced by North Atlantic Water, the Lomonosov Ridge that separates the two (LOMROG07PC04), where the Transpolar Drift is the strongest force, and Baffin Bay (IODP-EXP400U1606B and IODP-EXP400U1608A), where a lot of different currents come together (Fig.5). After the Lomonosov Ridge proved to be very fruitful for research of benthic foraminifera, another locality on the Lomonosov Ridge was chosen (LOMROG12PC03) to see if the same circumstances could be found and, as there is an existing age model for LOMROG12PC03 (Razmjooei et al., 2023), if an age could be assigned to the transition. Furthermore, Anne Jennings (Institute for Alpine and Arctic Research, University of Colorado) kindly provided already identified specimens from sites 93030-03BC (Southwestern Iceland Shelf), OD1507 (Nares Strait) and 200802959PC (Lancaster Sound) that were not only analysed but also used as an aid to identify the different species, alongside with the identification charts provided by the paper of Cage et al. (2021). The foraminifera used in this study were picked from already washed and sieved samples ($> 63 \mu\text{m}$). The samples were sprinkled evenly on a sample tray and analysed under the light microscope. If possible, only the best-preserved specimens were chosen for imaging. Of LOMROG07PC04 the whole core was available and proved extremely useful, hence at least five specimens from each 10 cm of depth (where foraminifera were present) were analysed. In the cores from IODP-EXP400 the samples were sieved again and only the size fractions between $63 \mu\text{m}$ and $250 \mu\text{m}$ were observed to increase the chance of finding foraminifera in the sediments. In total, 1031 foraminifera were imaged and analysed. Foraminifera exhibit a certain range of individual variation, therefore, where possible, always more than one specimen is presented to ensure that the results were representative of the whole sample/species and not only one exceptional individual.

As foraminifera are abundant in times of interglacials, only interglacial sediments were researched within the project. In the Arctic Ocean dark brown, bioturbated, finer-grained, Mn-enriched layers are characteristic of interglacial sediments (Jakobsson et al., 2000, O'Regan et al., 2008). This can also be witnessed in the sediments from the Lomonosov Ridge (O'Regan et al., 2008), here exemplified by core LOMROG07PC04 (Fig.7). The first 200 cm mainly contain slightly sandy dark-yellowish-brown mud that alternates with sandy lighter-yellow mud. Below 200 cm the mud becomes more and more mottled and below 300 cm it turns from sandy into silty mud. Many contacts are uneven, probably due to bioturbation (Jakobsson et al., 2008).

LOMROG07PC04 was chosen for most morphometric analyses because it showed an unusual amount of highly diverse benthic foraminifera, with an exceptional abundance of *Cassidulina*. The selection of sample depths in LOMROG07PC04 was based on the interglacials and glacials indicated by the lithography and the foraminifera counts from Hanslik (PhD thesis, 2011). In the other cores, where no core descriptions or foraminifera counts were readily available, each 10 cm depth interval was investigated to find interglacials. Additional factors after which samples were selected from all cores were abundance of specimens and state of preservation.

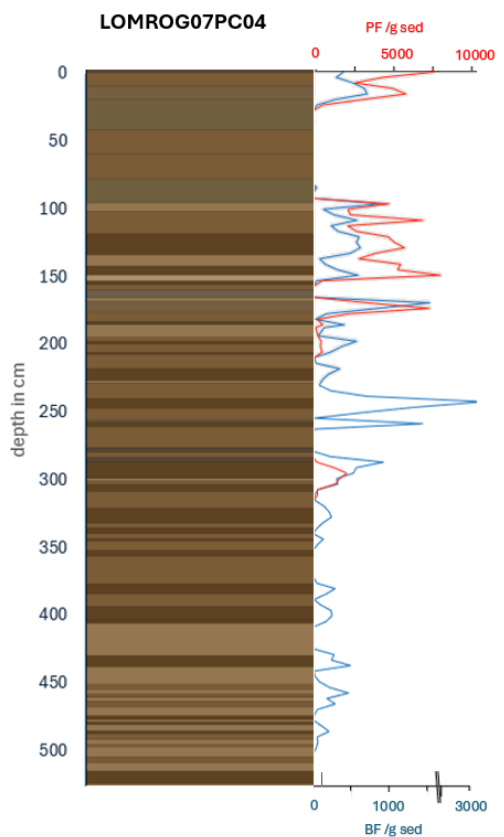


Fig.7: Lithography and foraminifera count from Core LOMROG07PC04. Marked in red are planktonic foraminifera per gram sediment, marked in blue are benthic foraminifera per gram sediment. Generally, darker sediment layers represent interglacials and lighter layers glacials, which are mostly barren of foraminifera.

Created from Jakobsson et al., 2008 and Hanslik, PhD thesis 2011.

2.2 Light microscope and SEM images

Light microscope images were taken with a LEICA M205 C microscope and the image capturing software LAS V 4.0. As the clear identification of apertural features was not possible through the light microscope, well-preserved representative specimens were chosen for Scanning Electron Microscopy (SEM). The short-wavelength electron beams allow a much higher resolution than the longer wavelength photons in a light microscope. Before analysis, those specimens were mounted on sticky carbon disks and gold coated using a JEOL JFC_1200 Fine Coater (2 × 60 seconds, applied current of 20 mA) to prevent charging of the sample surface, which can lead to a blurred image. The SEM analysis was performed using a Hitachi TM 3000 Tabletop Microscope at the department of Materials and Environmental Chemistry, SU.

2.3 Morphometrics

To find the *C.neoteretis/teretis* transition, up to 20 of the best-preserved specimens from different depths were compared based on their apertural structures. To narrow down the transition, additional samples of the crucial depth period between 146 cm and 197 cm were analysed, due to temporal limitations only five specimens of those depths could be included.

Following other papers analysing benthic foraminiferal morphometrics (e.g. Galeotti & Coccioni, 2001, Dumitriu et al., 2018, Santana et al., 2021) I determined the size by measuring test length and width (Fig.8). The samples were sprinkled evenly on a sampling tray and then all specimens of a determined area were picked and measured. Fragmented specimens were not considered. The digital measurements were based on the umbilical side light microscope images and executed manually using the ImageJ software. The length was measured as the largest diameter centralized through the umbilical boss and the width perpendicular at half length. 30 specimens of 18 samples were morphometrically analysed and the direction of coiling (sinistral or dextral) was recorded. To improve the measurement certainty, repetition of the measurement was performed multiple times, which yielded a variability of 6-8 μm at the same depth. Compared with the variations throughout the core this is a relatively small difference, it can therefore be assumed that the method gives an appropriate estimate of size variations with depth. The longest diameter of the umbilical boss of ten specimens from 17 samples were measured. Statistical calculations to test correlations of foraminiferal size to sediment depths were executed with <https://www.statskingdom.com/correlation-calculator.html>. For the measurement of pore sizes, SEM images with 6.000 times magnification were taken adjacent to the aperture on the umbilical side (Fig.8). Where it was possible, the greatest diameter of ten pores of every specimen was manually measured using ImageJ, five specimens of each sample were analysed. Pore size could only be measured in very well-preserved individuals.

In the results only the averaged numbers are shown, full data sets can be found in Appendix B.

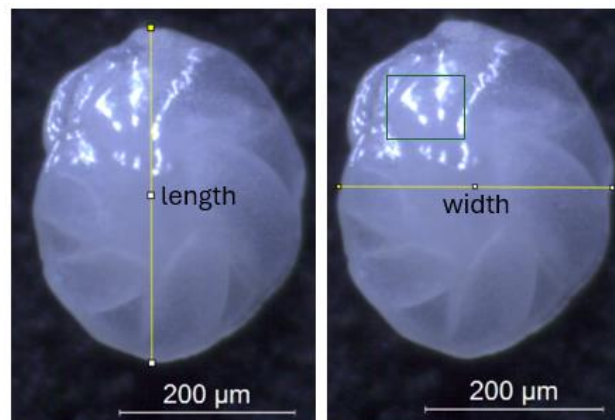


Fig. 8: Size measurements as performed with ImageJ. The green box marks the area from which pore size measurements were taken.

Results

3.1 Key characteristics of relevant benthic foraminifera

Six species as observed in this project are introduced in a more detailed way below, including: *Cassidulina obtusa*, *Cassidulina reniforme*, *Cassidulina cf. reniforme*, *Cassidulina laevigata* and finally *Cassidulina neoteretis* and *Cassidulina teretis*. In each case both light microscope and SEM images are presented. Except for *C. teretis*, the specimens presented here were provided and identified by Anne Jennings (Institute for Alpine and Arctic Research, University of Colorado).

C. obtusa from the Holocene on the Southwestern Iceland Shelf (93030-03BC) as viewed under the light microscope has an elongated aperture bordered by a thin lip flap (Plate 1) that shows

similarities to the aperture of *C. neoteretis* (Fig.2). The aperture is slit-like, and the apertural flap is smooth, slightly crenulated and shows no teeth. In the SEM however it becomes apparent that the apertural flap is generally thinner and longer than in other *Cassidulina* species, more comparable to the *Paracassidulina* group (Fig.6). The chambers are much more inflated than in any of the other regarded species, giving the chambers of *C. obtusa* an almost globular appearance. The average pore size of the specimens researched in this project is 0,49 μm (Appendix B1). As the features of *C. obtusa* are clearly distinguishable from other members of the group *Cassidulina* and *C. obtusa* prefers a boreal environment over the Arctic (Sejrup & Guilbault, 1980), it will not be further discussed in this thesis.

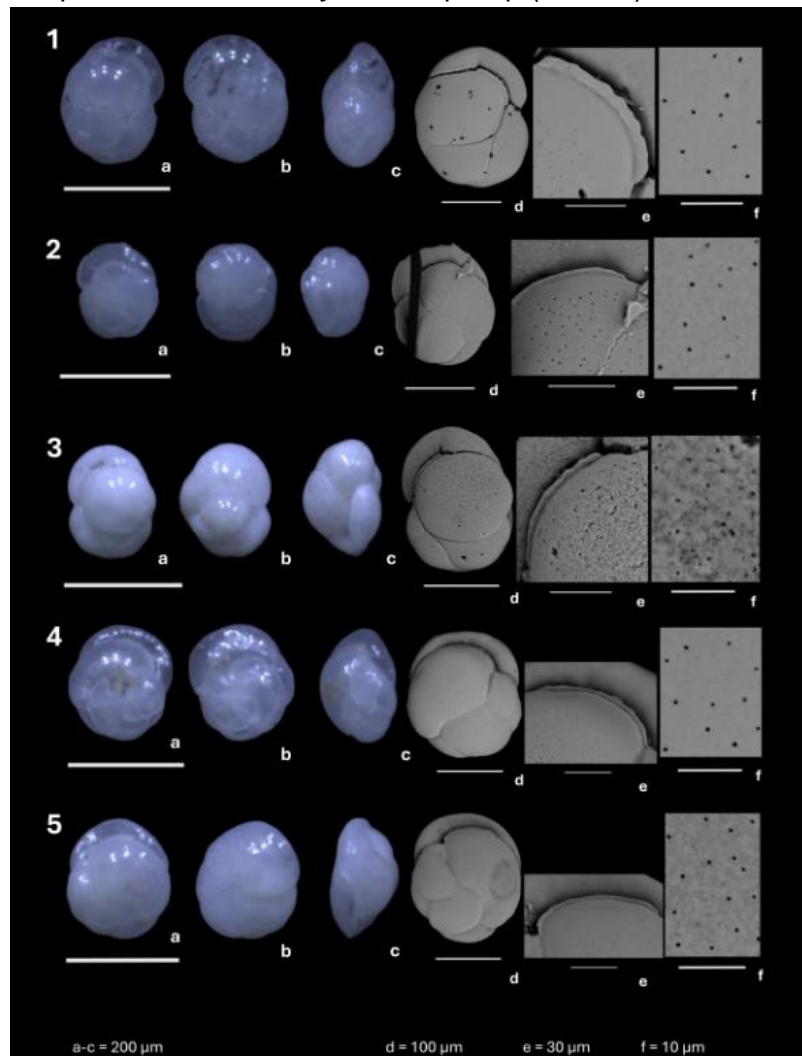


Plate 1: 1-5: Light microscope and SEM images of *Cassidulina obtusa* from Core 93030-03BC (Southwestern Iceland Shelf, Holocene) at 6-7 cm depth.

a = umbilical view, b = spiral view, c = lateral view, d = SEM umbilical view, e = SEM aperture f = SEM pores.

C. reniforme's most characteristic features are large chambers with sharp sutures that meet in the center, leaving no room for an umbilical boss (Plate 2). On the SEM images it often looks like the foraminifera is divided into four parts because of the distinct sutures. Typical is also the kidney-like rounded shape with slightly inflated chambers. The aperture is also slit-like and covered by a distinctive flap that is generally shorter and more crescent than in *C. neoteretis*. The edge of the flap is irregularly crenulated, but shows no clear teeth as in *C. laevigata* or *C. teretis*. The average pore size in the samples researched here is 0,73 μm (Appendix B2). The specimens presented here stem from Holocene/Late Pleistocene sediments gathered northwest of Greenland.

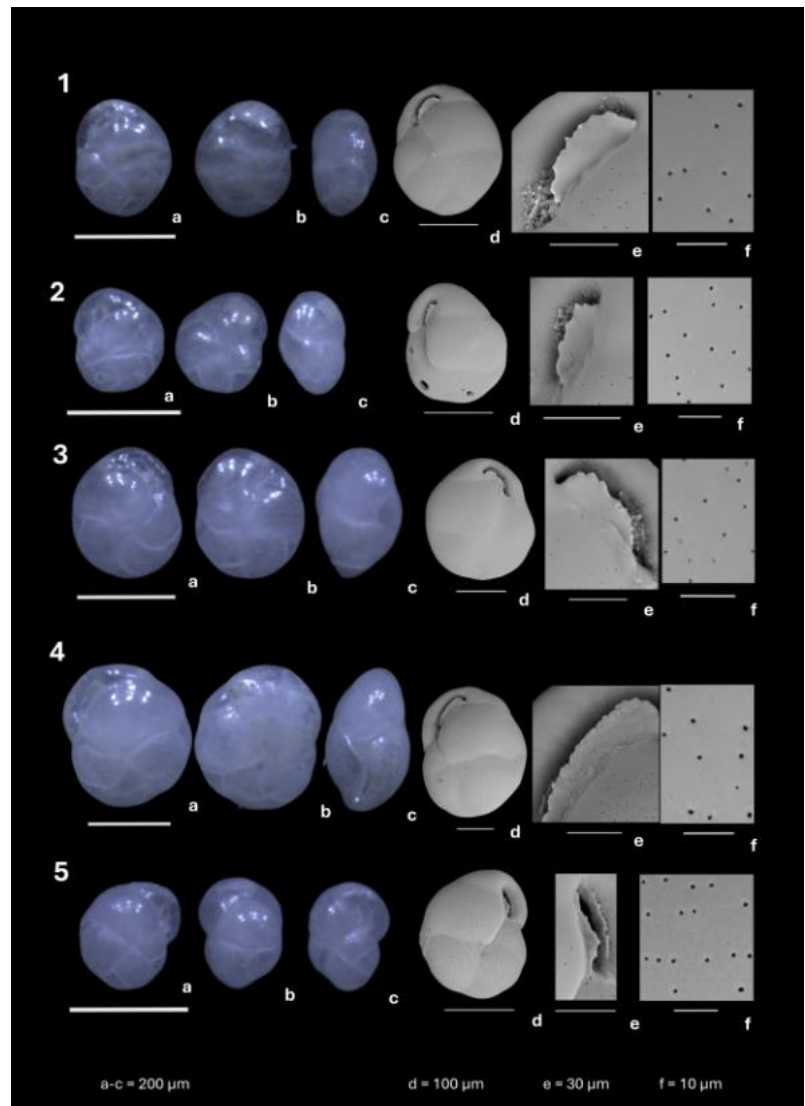


Plate 2: Light microscope and SEM images of *Cassidulina reniforme* from the Holocene/Late Pleistocene northwest of Greenland in Core: 1 + 2: 452T2 (same location as OD1507), 1 m above river; 3: 200802959PC 303-305 cm depth; 4: 200802959PC at 585-587 cm depth; 5: OD1507 at 72-74 cm depth. a = umbilical view, b = spiral view, c = lateral view, d = SEM umbilical view, e = SEM aperture, f = SEM pores.

C. cf. reniforme shares the rounded shape and the absence of an umbilical boss (Plate 3) with *C. reniforme*. It has distinctly sigmoidal sutures and is slightly more compressed than *C. reniforme*. The shape of the chambers differs from *C. reniforme*, with a twisting into a more angular shape towards the center. The aperture has a similar shape as *C. reniforme* but in contrast to *C. reniforme* the apertural flap of *C. cf. reniforme* has more clearly pronounced teeth. The apertural flap is contained between two semicircular incisions. The average pore size here is 1,14 μm (Appendix B3). All specimens of *C.cf reniforme* were found in samples from the Pleistocene in Baffin Bay.

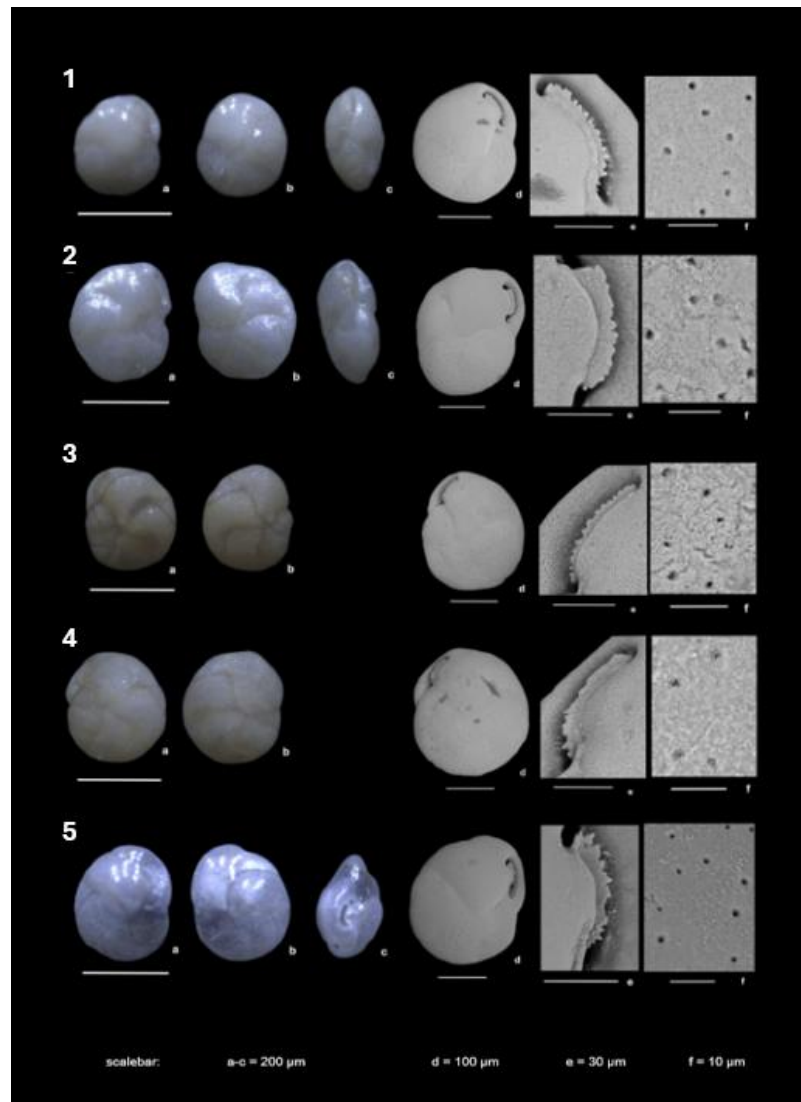
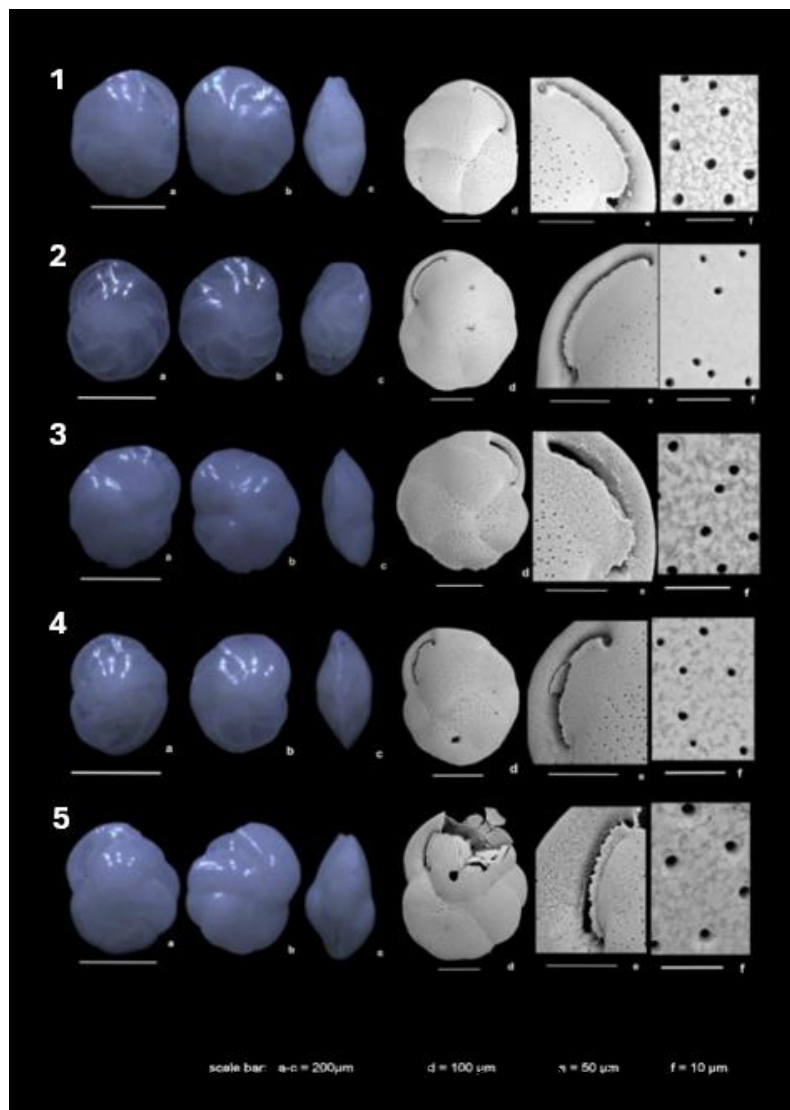


Plate 3: Light microscope and SEM images of *Cassidulina cf. reniforme* from the Pleistocene (below Brunhes-Matuyama boundary) in Baffin Bay in Core: 1+2: IODP Exp400-U1606A-11R-CC(Core Catcher), 3+4: IODP Exp400-U1606A-13R-CC, 5: IODP Exp400-U1606B-14R-CC.

a = umbilical view, b = spiral view, c = lateral view, d = SEM umbilical view, e = SEM aperture, f = SEM pores.

C. laevigata has large ovate and curved chambers interspersed with smaller subtriangular chambers; the large chambers meet in the middle, leaving no space for an umbilical boss (Plate 4 and Fig. 6). It is more laterally compressed than *C. reniforme* and *C. cf. reniforme*, pinching out at the periphery into a keel. The peripheral outline is slightly lobate. The aperture is crescent-shaped and longer than in other *Cassidulina* (except for *C. obtusa*) and the apertural plate shows fine, clearly pronounced teeth. An outstanding characteristic feature is the large pore size, here 1,58 μm on average (Appendix B4). The specimens presented here stem from Holocene sediments on the Southwestern Iceland Shelf (93030-03BC).



from Holocene in the Southwestern Iceland Shelf in Core 93030-03BC at 6-7 cm depth. Specimen 5 was damaged during preparation for the SEM.

a = umbilical view, b = spiral view, c = lateral view, d = SEM umbilical view, e = SEM aperture, f = SEM pores.

C. neoteretis usually has eight to ten chambers arranged in four to five pairs, alternating between a larger rounded chamber reaching onto the umbilical boss and a smaller subtriangular one (Plate 5, Fig.2 and 6). The umbilical boss is predominantly milky or semitranslucent and free from pores. The peripheral outline is lobular, almost crenulate. The test is laterally compressed, pinching out into a refined keel, giving the whole test a “Chinese dumpling”-like look. Parallel to the final chamber lies the elongated aperture that is partly covered by a smooth subtriangular apertural plate. The length of the aperture and its apertural plate can vary from elongated (Plate 5, Figs. 2e-4e) to short (Pl. 5, Fig. 5d-e). The average pore size is 1,08 μm (Appendix B5). The specimens presented here stem from Holocene sediment samples gathered northwest of Greenland.

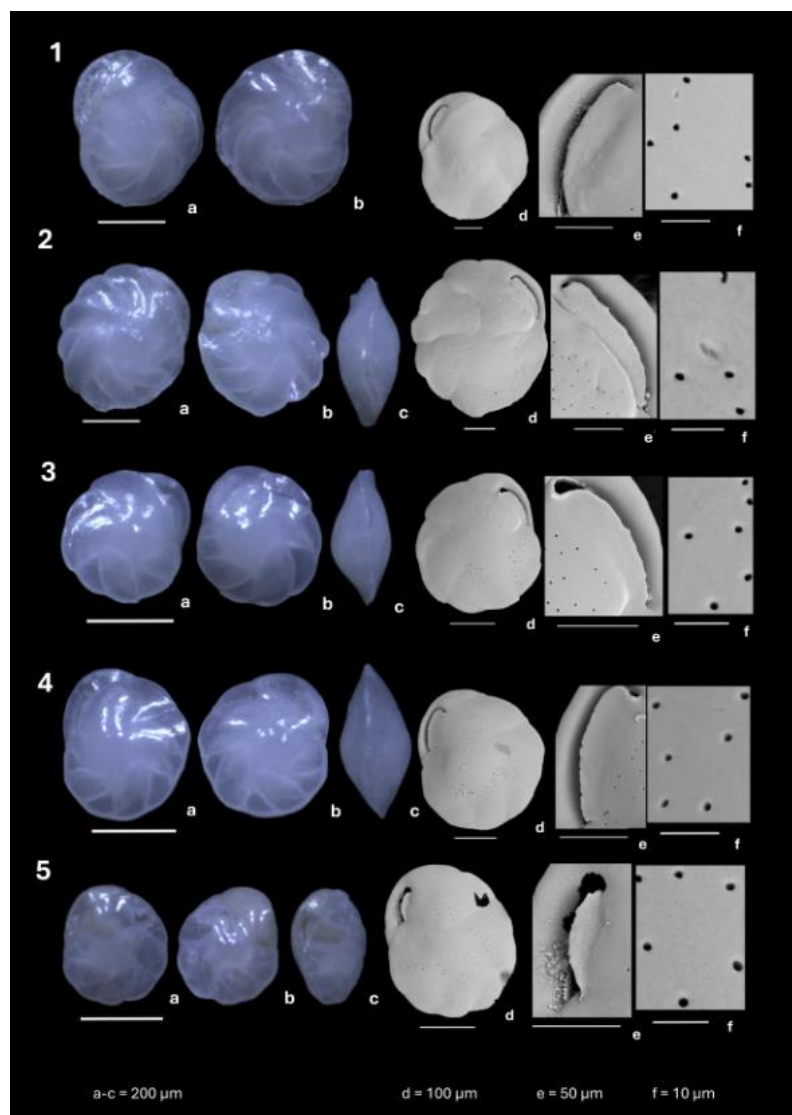


Plate 5: Light microscope and SEM images of *Cassidulina neoteretis* from the Holocene, northwest of Greenland in Core: 1-4: 200802959PC at 303-305 cm depth, 5: OD1507 at 72-74 cm depth. a = umbilical view, b = spiral view, c = lateral view, d = SEM umbilical view, e = SEM aperture, f = SEM pores.

C. teretis has the same shape and chamber arrangement as *C. neoteretis* (Plate 6). The observation made by Cage et al. (2021) that *C. neoteretis* typically has a blunter end of the chambers towards the umbilical boss compared to *C. teretis* having more rounded chambers could not be confirmed in this study. Qualitative assessment showed that the shapes of chambers vary more by individual than by species. The umbilical boss especially in older specimens can sometimes be bulked out. The most prominent difference from *C. neoteretis* lies in the aperture, which has a serrated crescent-shaped apertural plate. The apertural plate and its edge ornamentation is the most elaborate of the *Cassidulina* morphotypes discussed here. It is laterally wider than in the other species and the teeth are more angular. Some specimens possess a row of counter teeth on the opposite side of the apertural slit (Plate 6, Figs. 3e and 4e). Remains of a row of counter teeth can sometimes also be found in *C. neoteretis* (Plate 5, Fig.5e). Another difference from *C. neoteretis* was found in the size of the pores, which is 0,52 μm on average in the samples of this project (Appendix B6). The specimens portrayed here stem from Pleistocene sediments of the Lomonosov Ridge.

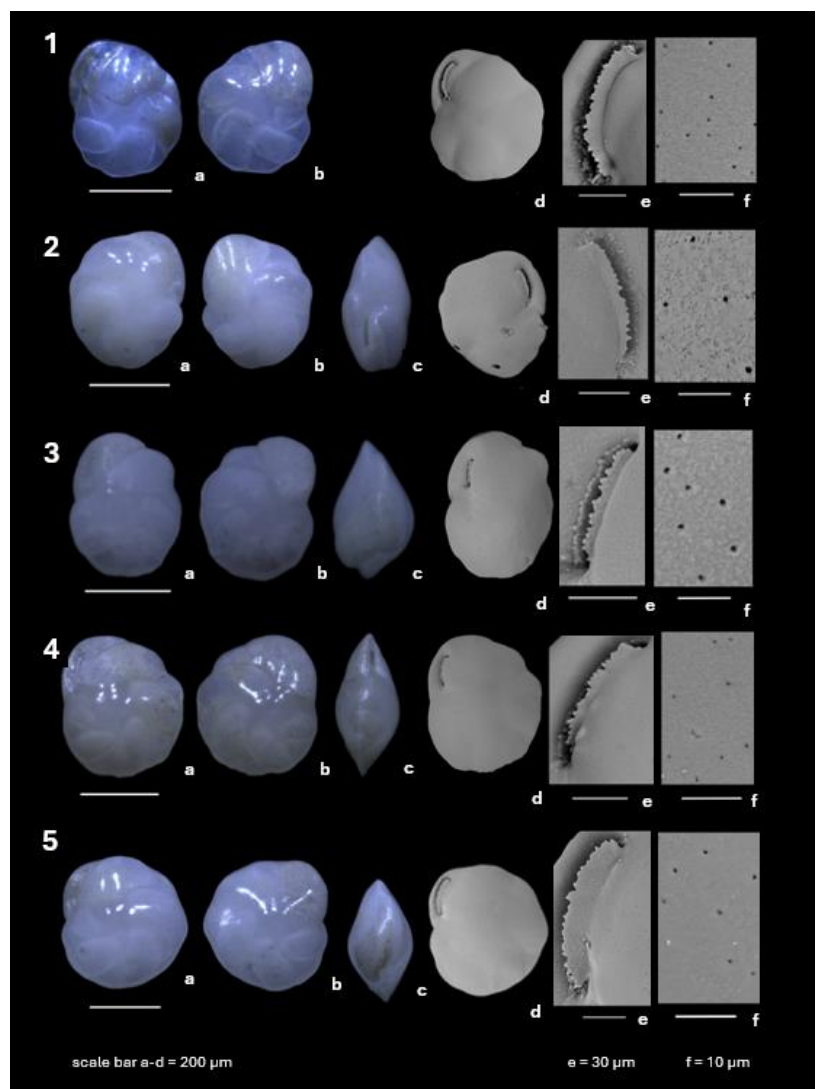


Plate 6: Light microscope and SEM images of *Cassidulina teretis* from the Pleistocene in the Lomonosov Ridge in Core: 1: LOMROG07PC04 at 301 cm depth, 2: at 459 cm depth, 3: LOMROG12PC03 at 172 cm depth, 4: at 211 cm depth, 5: LOMROG07PC04 at 197 cm depth. a = umbilical view, b = spiral view, c = lateral view, d = SEM umbilical view, e = SEM aperture, f = SEM pores.

3.2 Changes through time in Core LOMROG07PC04

Using the above definitions for *C. neoteretis* and *C. teretis*, the apertural flaps of specimens from each sample were assigned to the categories smooth, undetermined, and serrated. All specimens that could not be clearly placed, due to poor preservation or a transitional shape of the apertural flap, were categorised as undetermined. A clear transition from *C. neoteretis* to *C. teretis* based on the morphology of the apertural plate can be observed in Core LOMROG07PC04 (Fig.10). The last depth where it was possible to identify *C. neoteretis* was 171 cm, whereas the first depth that contained exclusively *C. teretis* was at 183 cm. Samples in between were barren or contained only few so poorly preserved specimen that no identification was possible. Nonetheless, the results are striking. All well-preserved specimens above 171 cm show smooth apertures and can with great certainty be identified as *C. neoteretis* except for one, that still had teeth, being the absolute exception. All well-preserved specimens below 183 cm show clear teeth and can be identified as *C. teretis*. It needs to be mentioned that many samples were suffering from poor preservation. No gradual change was observed, but a clear change from smooth to serrated apertures (Plate 7). The changeover from *C. neoteretis* to *C. teretis* must have happened between 171 cm and 183 cm depth.

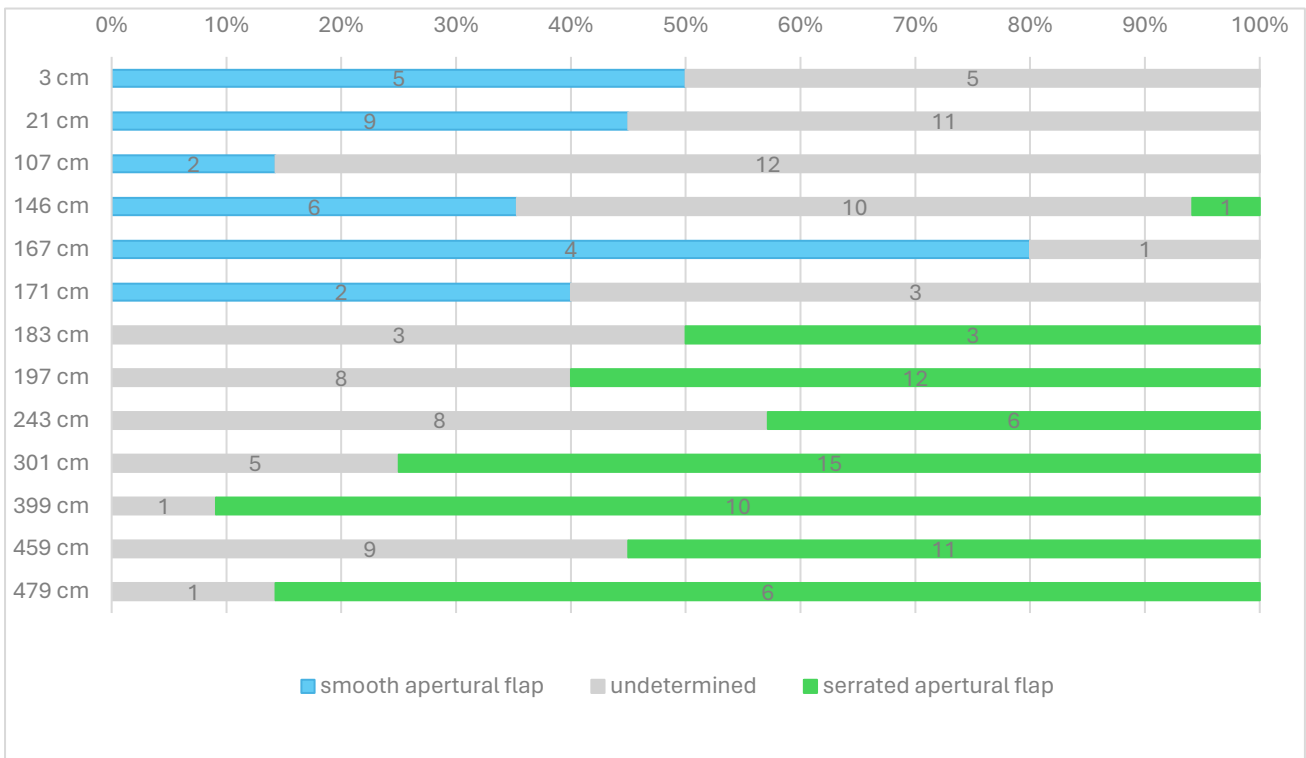


Fig.10: Percentage of smooth/serrated apertural flaps of specimens of *C. neoteretis/teretis* throughout Core LOMROG07PC04 (Appendix B7). All specimens that could not be clearly assigned to one or the other were labelled undetermined. Between 5 and 20 specimens per depth were analysed.

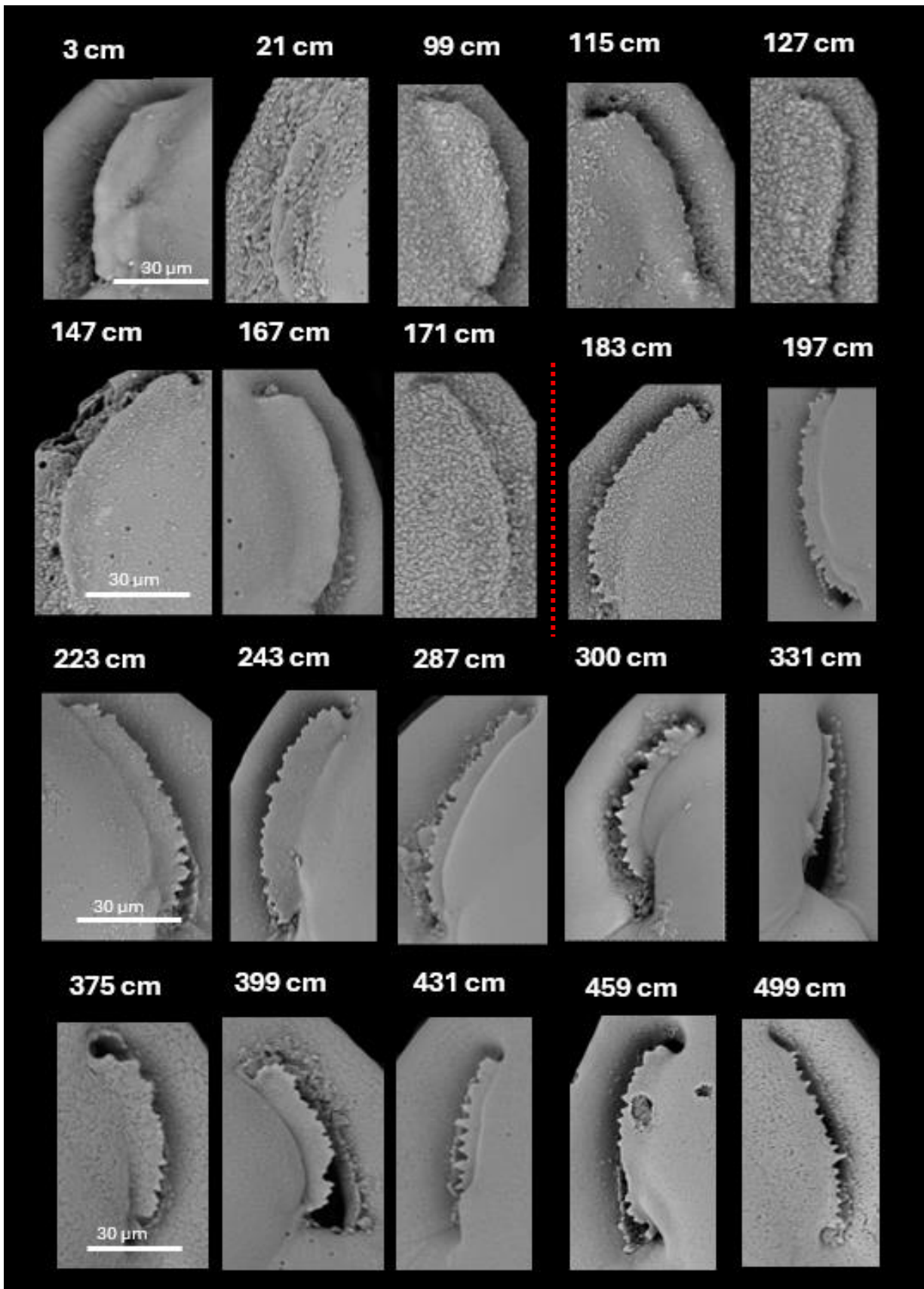


Plate 7: Change in morphology of the apertural flap in Core LOMROG07PC04. The red dotted line marks the transition from *C. neoteretis* with a smooth subtriangular apertural flap to *C. teretis* with a more crescent apertural flap with prominent teeth. Despite poor preservation at 171 cm depth, the smooth subtriangular shape of the apertural flap can be seen. Scale bar applies to whole row.

The length-width ratio of the tests oscillated only slightly between samples (between 1,15 and 1,22), showing that the shape remains similar through time, so length alone should be a good indicator of changes in size. The diameters of *C. neoteretis*/*C. teretis* in LOMROG07PC04 lie between 149 and 664 μm (Fig.11). Those are however the extreme examples; the average lies at 311 μm . Because of the great outliers, using the median was investigated as well, but proved to not differ significantly from the mean. As becomes clear when looking at the results (Fig.11), the size oscillates greatly. Even though an increase in size was witnessed through qualitative assessment, the quantitative acquisition of data showed that the mean length rises and falls quite rapidly throughout the core. It can however be observed, especially when looking at the minimum and maximum lengths, that even though the minimum length stays in a similar frame, there is a general trend towards larger specimen with increasing depth. It was not possible to distinguish *C. neoteretis* from *C. teretis* or to find the transition solely based on the diameter of the specimens, however, results of the spearman correlation indicated that there is a significant small positive relationship between test diameter and depth, $r(538) = .14$, $p = .001$. The spearman correlation was used because the measured specimens did not display normal distribution due to extremely large outliers. The size of the umbilical boss had a significant large correlation towards the size of the test, $(r_{15}) = .606$, $p = 0.10$, but a non-significant correlation towards depth, $r(15) = .478$, $p = .855$. For the umbilical boss sizes, the values showed normal distribution, hence the pearson correlation was calculated.

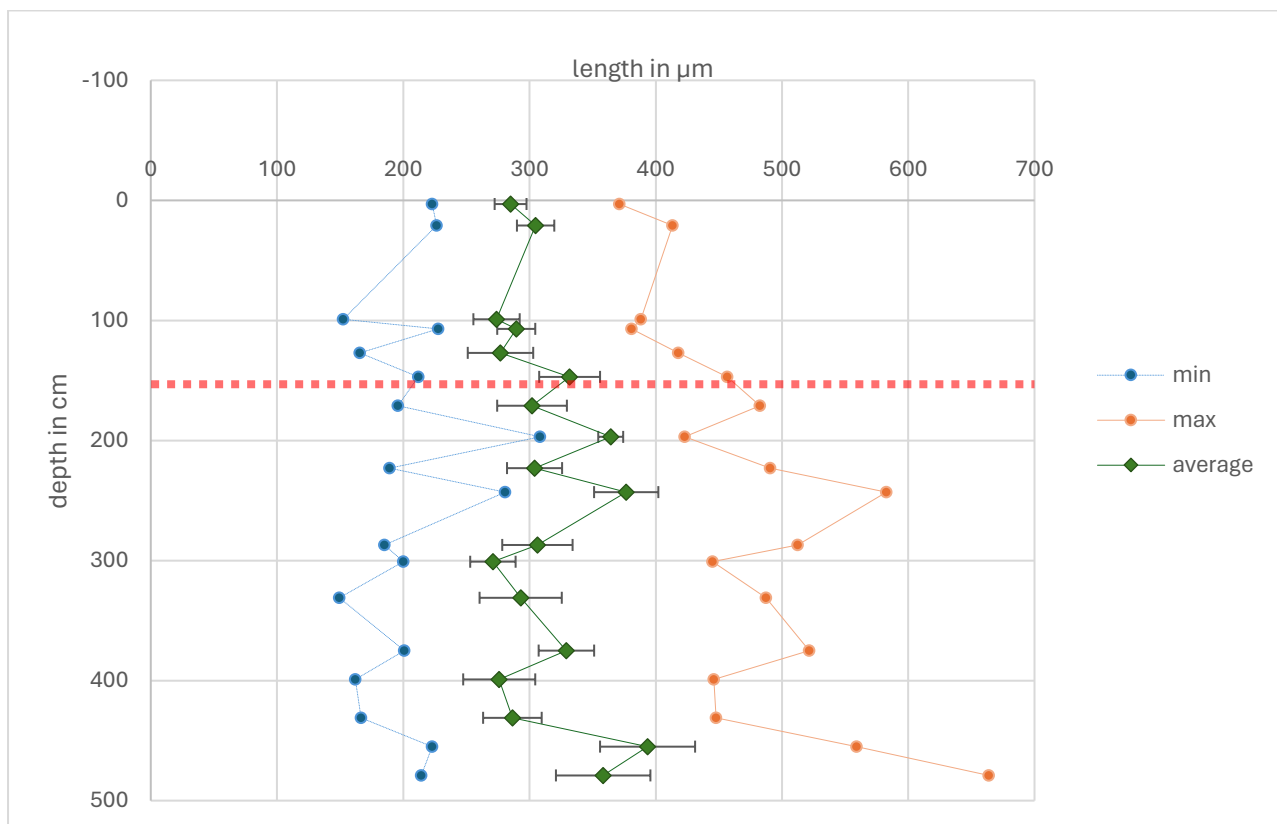


Fig.11: The minimum, maximum and mean diameter of *C. neoteretis/teretis* in Core LOMROG07PC04 (Appendix B8). The error bars show the standard error of the mean. The red dotted line marks the depth of the *C. neoteretis/teretis* transition.

The pore sizes of LOMROG07PC04 clearly reflect the transition from *C. neoteretis* to *C. teretis* (Fig.12). Whereas the mean pore diameter above 167 cm depth ranges between 0,73 μm and 0,80 μm , below 183 cm depth it ranges between 0,45 μm and 0,57 μm . The difference is so large that it is even visually detectable in the SEM images (see Plate 5 and 6).

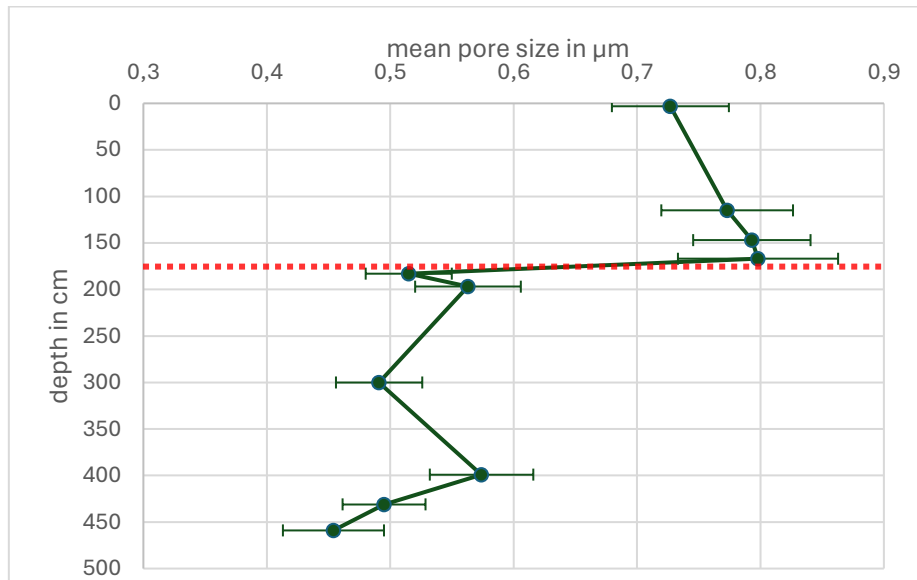


Fig.12: Mean pore diameter of *C. neoteretis/teretis* in core LOMROG07PC04 (Appendix B9). The error bars show the standard error of the mean (Appendix B10). The red dotted line marks the depth of the *C. neoteretis/teretis* transition.

Another parameter researched was the direction of coiling. The distribution of left (sinistral) and right (dextral) coiling individuals was relatively even, with a slight trend toward sinistral coiling (Fig.13). In total, *C. neoteretis* shows a tendency towards sinistral coiling of 58 %, whereas *C. teretis* shows a tendency towards sinistral coiling of 54 %. The direction of coiling proved not relevant for species determination.

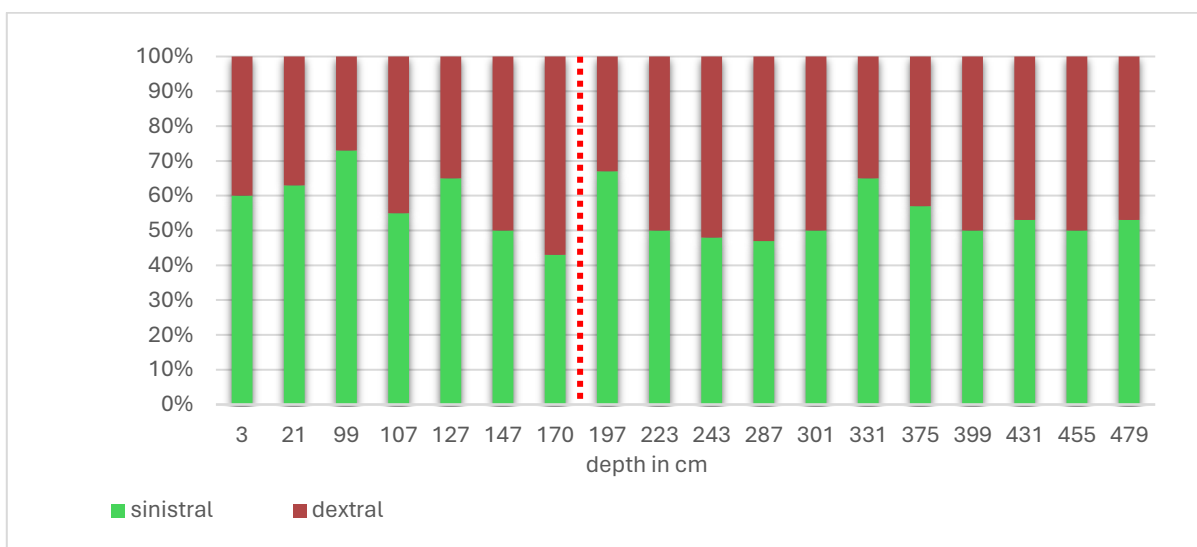


Fig.13: Percentages of coiling direction of *C. neoteretis/teretis* in Core LOMROG07PC04 (Appendix B10). The red dotted line marks the *C. neoteretis/teretis* transition.

3.3 Morphological variability

Even though the key characteristics of *C. neoteretis* and *C. teretis* are consistent, each and every individual specimen looks different. The size, shape, direction of coiling and (in this case of special interest) the morphology of the aperture are important features in taxonomic identification. A complication in that field is that they can vary to a certain extent, even within the same sample (Plate 8 and 9). The size, the arrangement and shape of the chambers, and the lobation and pinching of the peripheral outline have been witnessed to differ between individual specimens. Not every specimen of *C. neoteretis* has a perfectly smooth aperture, some still have remnants of teeth, small bumps or an opposing row of teeth. The same is the case for *C. teretis*, where some do not have the perfectly serrated aperture, but a more bumpy or clean appearance. It was not always possible to differentiate between *C. neoteretis* and *C. teretis* looking at one individual but looking at the variability within one sample, a clear trend towards one or the other was always observable (Plate 10).

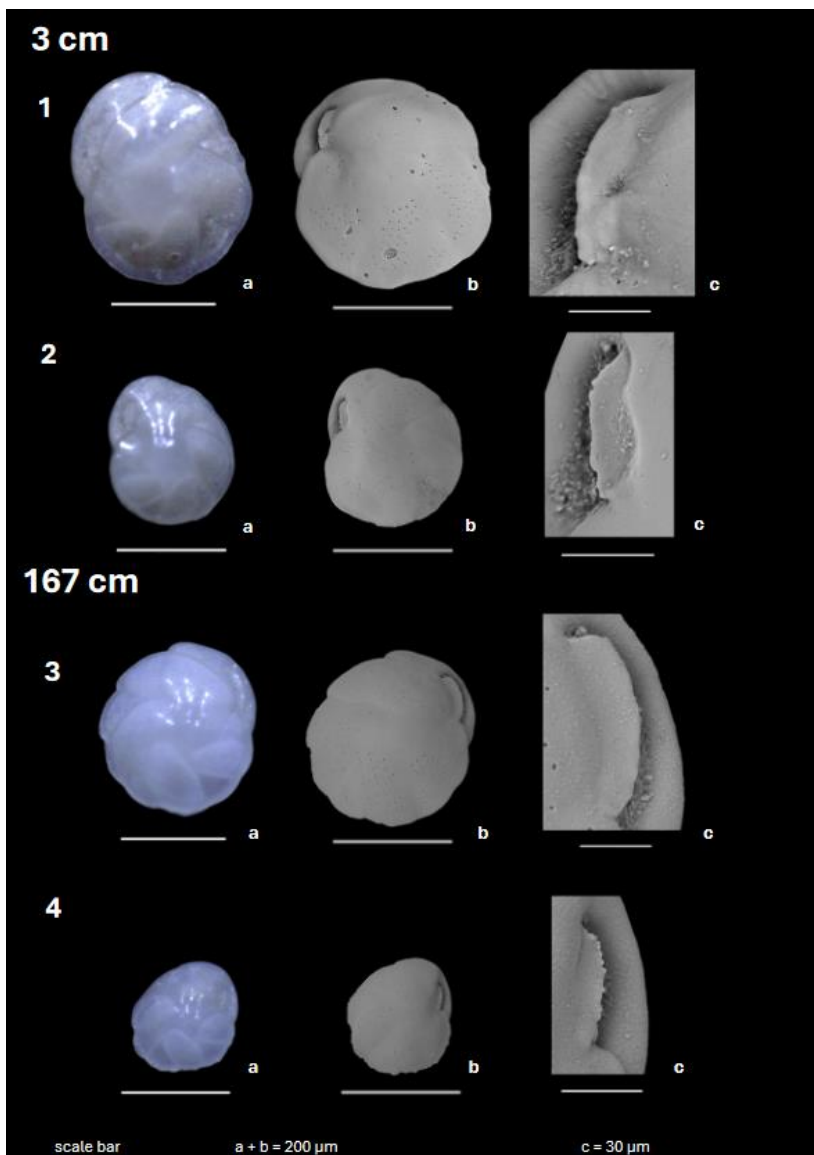


Plate 8: Range of variability between different specimens of *Cassidulina neoteretis* within Core LOMROG07PC04.

1+2: 2-3 cm depth, 3+4: 166-167 cm depth.

a = umbilical view, b = SEM umbilical view, c = SEM aperture.

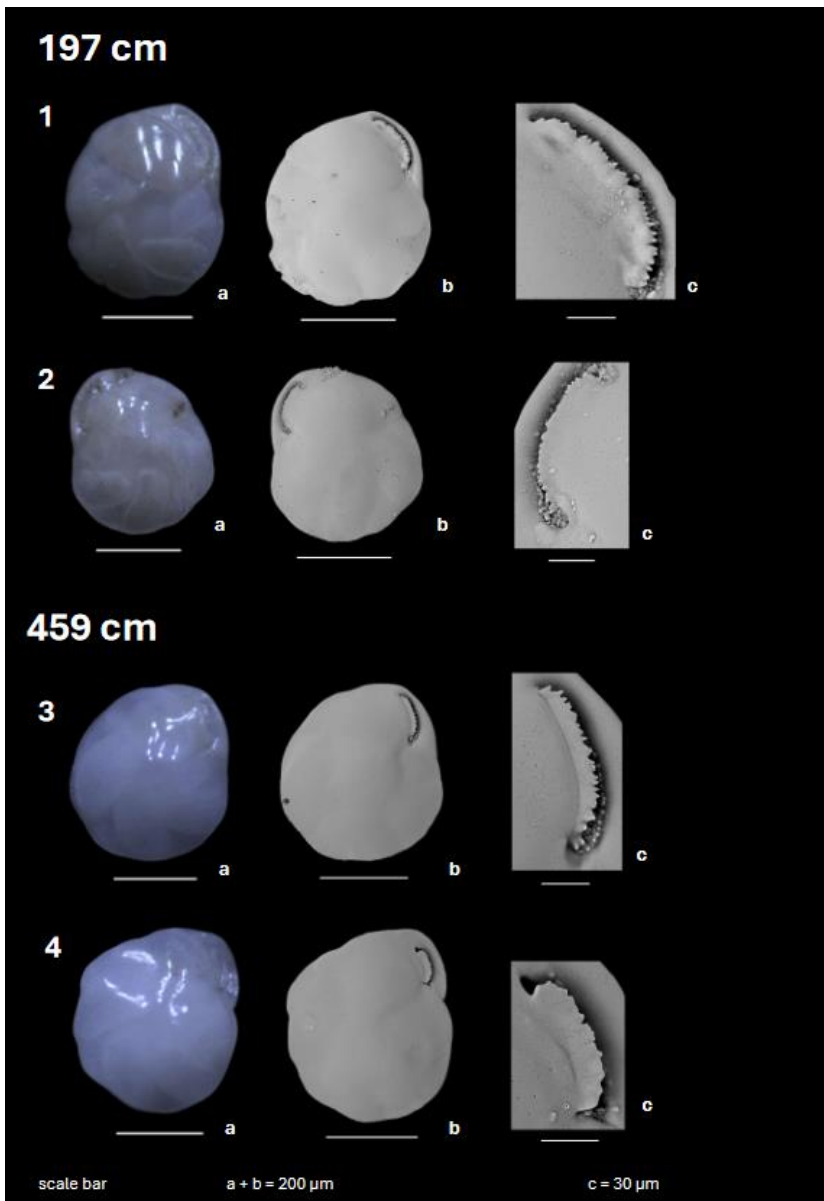


Plate 9: Range of variability between different specimens of *Cassidulina teretis* within Core LOMROG07PC04.

1+2: 196-197 cm depth, 3+4: 458-459 cm depth.

a = umbilical view, b = SEM umbilical view, c = SEM aperture.

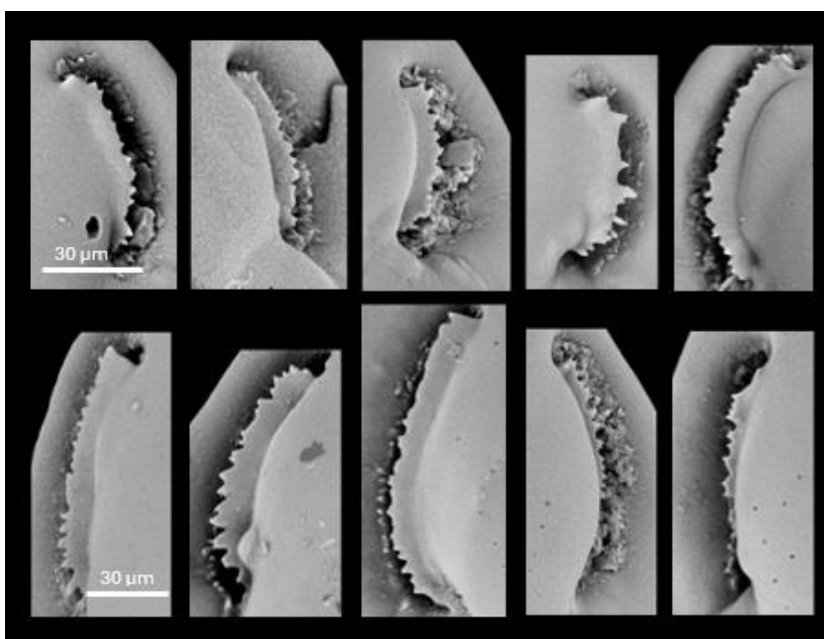


Plate 10: Range of variability between apertures of *Cassidulina teretis* within the same sample, LOMROG07PC04, at 300-301 cm depth. Some teeth are more extensive than others, but the total range shows clear serration of the apertural flap. These specimens display an exceptional state of preservation. Scale bars apply to whole row.

3.4 Comparison with LOMROG12PC03

Core LOMROG12PC03, lying approximately 100 km northeast of LOMROG07PC04, showed a much lower abundance of benthic foraminifera. Nonetheless, it was possible to detect the transition from *C. neoteretis* to *C. teretis* here as well (Plate 11). Until 127 cm depth, all well-preserved specimens were identified as *C. neoteretis*, whereas below 142 cm depth, all well-preserved specimens were identified as *C. teretis*. The transition therefore can be assumed to have taken place in LOMROG12PC03 between 127 cm and 142 cm depth.

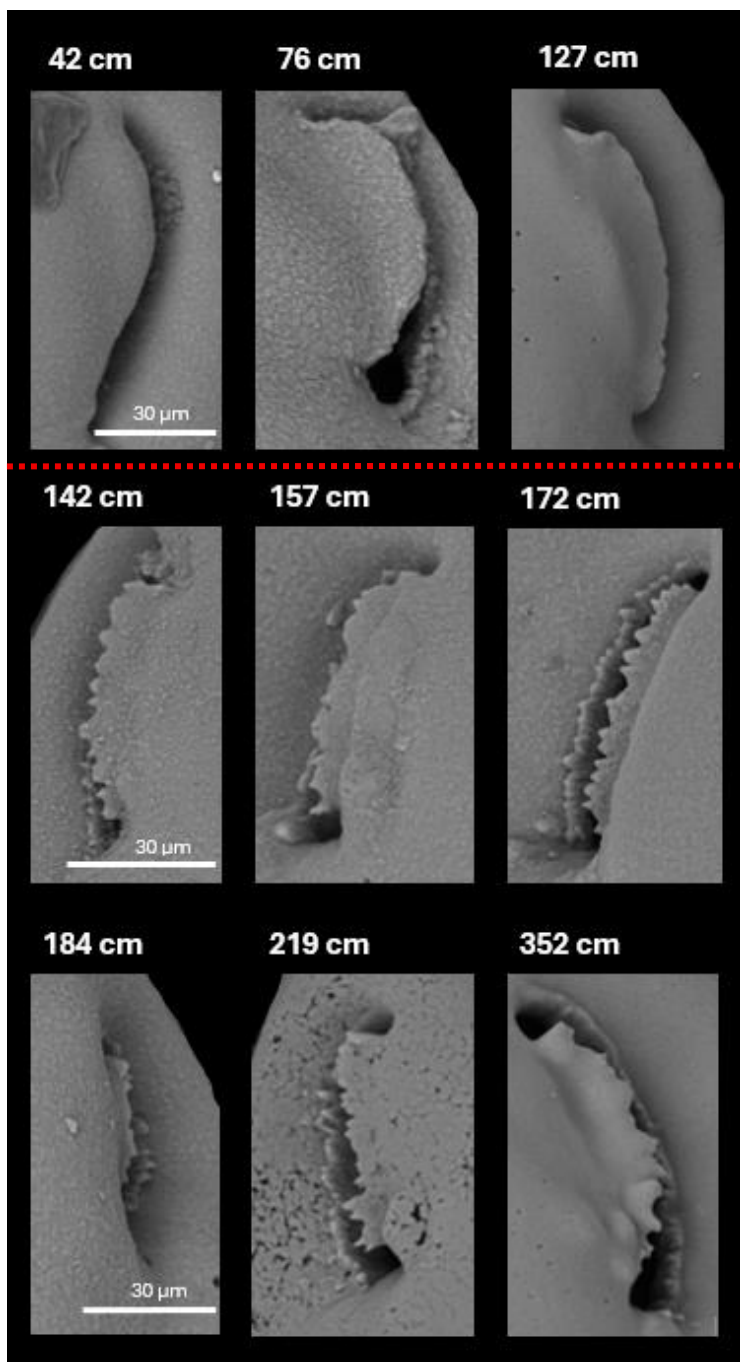


Plate 11: Change in morphology of the apertural lip in Core LOMROG12PC03. The red dotted line marks the transition from *C. neoteretis* to *C. teretis*. Scale bar applies to whole row.

3.5 Observations from other regions

From the other cores only few samples were available, but no downhole sequence, so only one of the two species was found. The only exception is AO16-8GC, in which no *Cassidulina* were encountered at all. Accordingly, in ODP Leg104-642B, SO2153Bx11, OD1507 and 200802959PC, following the beforementioned criteria of identification, only *C. neoteretis* was observed. The morphological variations were similar in different regions. It could be observed that *C. neoteretis* from the Norwegian Sea (Plate 12,1) have a more rounded outline and pointier chamber ends compared to the specimens from the Lomonosov Ridge (Plate 12, 5+6) which show a more carinated outline and a fairly rounded chamber shape. The variability within samples was mostly comparable to the variability between different cores.

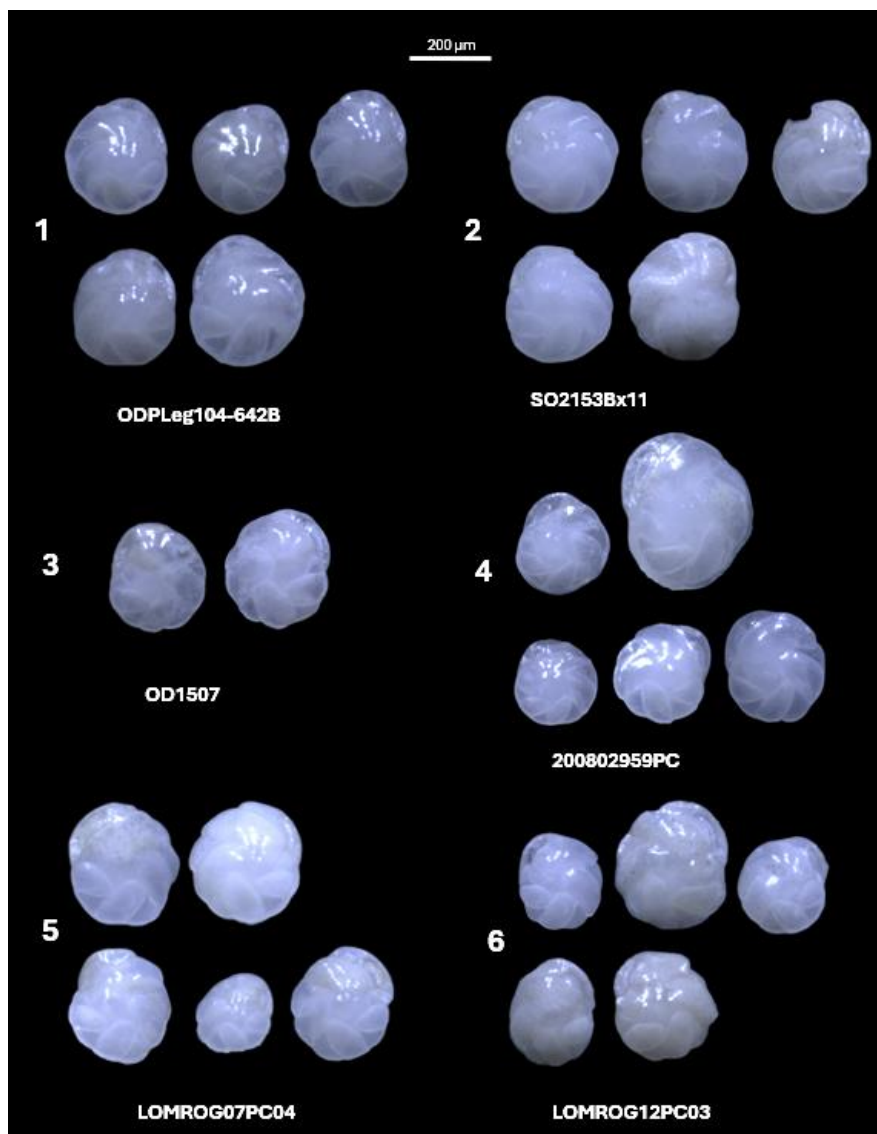


Plate 12: Light microscope images showing the regional variability of *C. neoteretis*. 1: ODPLEG104-642B (Norwegian Sea) at 104 cm depth, 2: SO2153BX11 (Northern Greenland) at 30 cm depth, 3: OD150703uw (Northwestern Greenland) at 74 cm depth, 4: 200802959PC (Lancaster Sound) at 305 cm depth, 5: LOMROG07PC04 at 167 cm depth, 6: LOMROG12PC03 at 127 cm depth (5+6: Lomonosov Ridge).

From the IODP EXP400 Cores U1606B and U1608A from Baffin Bay only a very low number of benthic foraminifera could be acquired which also were poorly preserved and did not give many clear results. The few identified specimens belonged to *I. norcrossi*, *C. cf. reniforme*, *C. laevigata* or *C. teretis* (of which the last two were often impossible to differentiate). The bulky prominent umbilical boss as well as teeth-like structures revealed by close-up SEM images of the apertural plate (Plate 13) lead to the classification of all possible *C. neoteretis/teretis* candidates in Core IODP EXP400-U1608A (below 9R-CC) as *C. teretis*. No foraminifera samples from more recent sediments in this area were available. The teeth were not as clearly pronounced as in other cores and the serration could also be the result of poor preservation. From most sample depths only one specimen was in a state of preservation that allowed interpretation and it cannot be assumed that one specimen is representative of the whole population. Due to the poor preservation state, pore sizes could not be analysed. Qualitative assessment showed that the benthic foraminifera in Baffin Bay were generally smaller in size than at the other cores researched in this project.

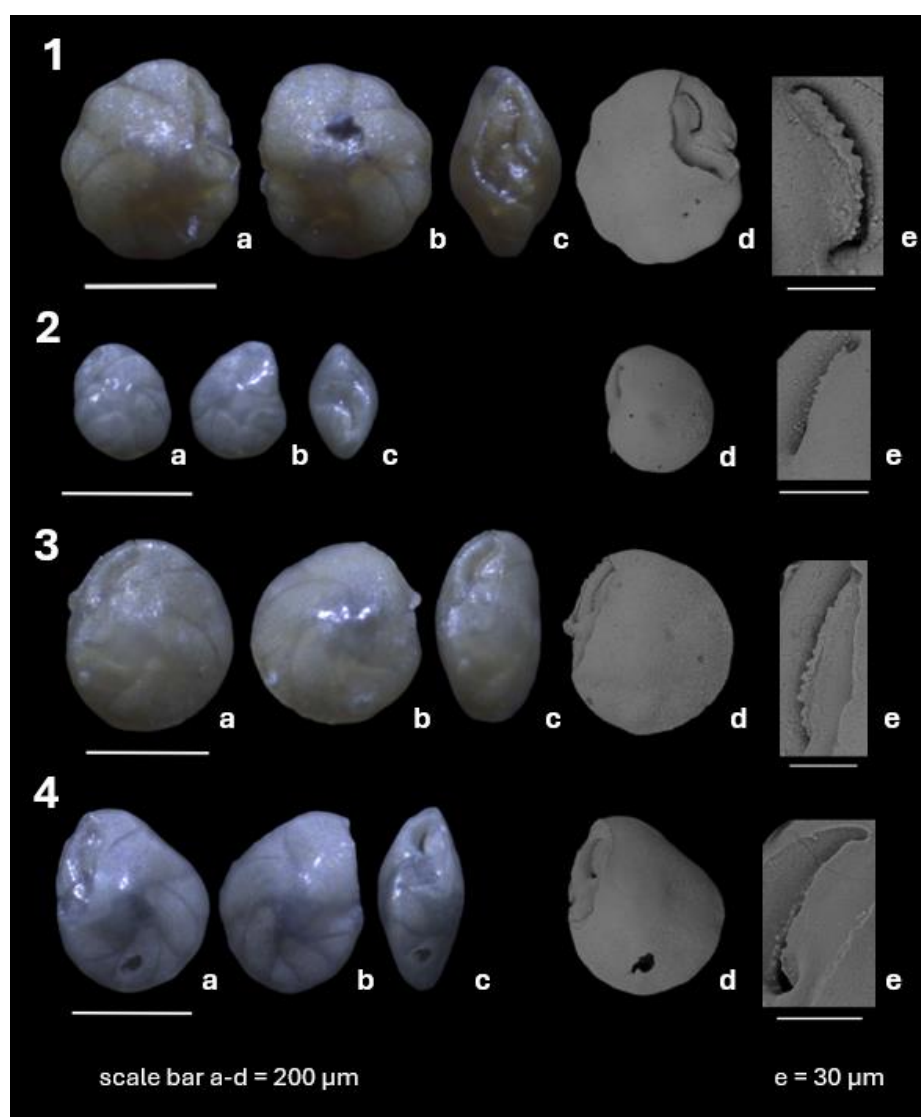


Plate 13: Light microscope and SEM images of *C. teretis* from Core IODP EXP400-U1608A-
 1: 33R-CC, 2: 36R-CC, 3: 44R-CC, 4: 48R-CC.
 a = umbilical view, b = spiral view, c = lateral view, d = SEM umbilical view, e = SEM aperture.

Discussion

4.1 From *teretis* to *neoteretis*

It was possible on a multitude of occasions to distinguish between *C. neoteretis* and *C. teretis* by looking at the morphology of the aperture, as the apertural flap shows either a crescent shape with teeth (*C. teretis*) or a smooth subtriangular shape (*C. neoteretis*). This confirms that the shape of the apertural flap is a valuable key characteristic for taxonomic differentiation between the two species. The test sizes however were fluctuating fundamentally, indicating that other factors such as the abundance of food or water temperatures have a larger influence on growth than the taxonomy. Even though the test diameters per depth did not give any specific indications and it would not be possible to tell the two species apart simply by looking at the sizes, a small positive statistical correlation between size and depth could be detected, proving that they were decreasing in size over time. If one looks at all of *C. neoteretis* and *C. teretis* as distinguished through the apertural features, the average diameter of *C. neoteretis* in core LOMROG07PC04 is 291 μm , whereas the average diameter of *C. teretis* is 323 μm . This confirms Seidenkrantz (1995) who observed in the North Atlantic and the Norwegian Sea that *C. neoteretis* averages between 260 μm and 300 μm and is generally smaller than *C. teretis*. It does however not fit into the original description from Tappan (1951), who described *C. teretis* to range between 360 μm and 550 μm . Tappan researched specimens from the Pleistocene in the Gubik Formation in Northern Alaska, so the difference could be caused by regional variations. According to Cage et al. (2021) *C. teretis* generally has a larger umbilical boss. This was briefly looked into, but only a significant correlation from the size of the umbilical boss towards the test size, not towards depth, was observed in this study. Even though that means a slight increase in the diameter of the umbilical boss in *C. teretis*, no concrete evidence toward this being species-dependent was found. The general shape of the umbilical boss that often was more bulked out and prominent can give a hint towards *C. teretis* as regarded under the light microscope, but on its own is not enough for a confident identification. Observing the direction of coiling gave no significant new insights, the slight increase in tendency towards sinistral coiling of *C. neoteretis* might be interesting but has no further implications.

An unexpected differentiation possibility between the two species was found in the pore sizes. The pore diameters in *C. teretis* were reliably smaller than *C. neoteretis* and could in some cases where the aperture was not helpful be used as a confirming parameter in identifying the species. In the paper of Seidenkrantz (1995) some of the SEM images seem to confirm this observation (Fig.14), suggesting that this is not only a regional phenomenon, but generally tied to the morphotype. However, in her paper no clear trend as found in this study is visible or described. Further research is necessary to prove that pore size could be added as a general distinction feature between those two species.

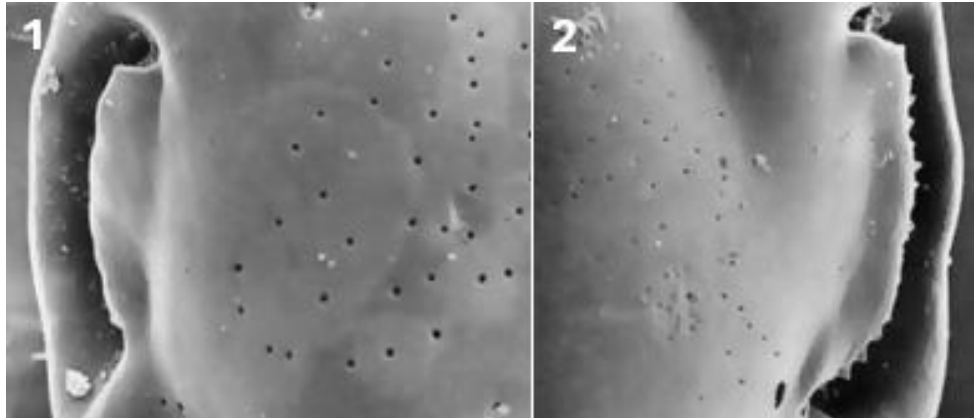


Fig. 14: Comparison of apertural shape and pore sizes. 1: *C. neoteretis* from the Upper Weichselian, Boring 1007 south of the Faeroe Island (MGUH no. 22216), X550; 2: *C. teretis* from the Upper Pliocene at DSDP Hole 552A (MGUH no. 22222), X500. Taken from Seidenkrantz (1995).

In general, the porosity of foraminifera is primarily related to test size as well as habitat temperature, where the pores increase with increasing test size and warmer temperatures (Burke et al., 2018). In benthic foraminifera however, the pore size is largely related to gas exchange intensity (Petersen et al., 2016). *C. teretis* tends to be larger in test size and lived in warmer conditions, but the pore size is significantly smaller, suggesting that gas exchange is the crucial factor here. Larger pore sizes mean a higher efficiency in oxygen intake (Wang et al., 2023), which would prove useful in oxygen-depleted conditions. It can therefore be postulated that during the transition from *C. teretis* to *C. neoteretis* the oxygen levels at the sea floor significantly decreased.

4.2 Signs of a cooling climate

That the *C. neoteretis/teretis* transition exists has been well established by Seidenkrantz (1995) for the North Atlantic and the Norwegian Sea and this study establishes it for the Lomonosov Ridge, supporting the value of distinguishing the two species, which are likely linked to changing environmental conditions. Cage et al. (2021) brought forward that *C. teretis* preferred warmer and shallower water, whereas *C. neoteretis* flourishes in cool stable water masses in the Arctic and subarctic. A possible explanation for the extinction of *C. teretis* and the evolution of *C. neoteretis* could be a cooling of the climate and increasing perennial sea ice cover. This would have a considerable influence on benthic foraminifera as it impacts the type and/or seasonality of food arriving at the seafloor. Data from Hanslik (PhD thesis, 2011) about the abundances of foraminifera in Core LOMROG07PC04 reveals that the *C. neoteretis/teretis* transition coincides with a shift between foraminiferal assemblages (Fig. 15). What immediately strikes the eye is that together with *C. teretis*, *Epistominella exigua* disappears from the core record, which in high abundances suggests enhanced primary production in surface waters (Hanslik, PhD thesis, 2011). *E. exigua*, that almost always coexists with *C. teretis* in Core LOMROG07PC04 (Fig. 15), is associated with mostly seasonal sea ice and a bloom in phytoplankton (Lazar et al., 2016),

allowing the conclusion that the summer sea ice cover in the time of *C. teretis* must have been much less severe than it is today. Shortly after *C. neoteretis* the Arctic species *Oridorsalis tener* and *Bulimina aculeata* appear, which suggest a dominating perennial sea ice cover (Hanslik, PhD thesis, 2011). *O. tener* commonly occurs in the present in sea ice covered areas of the central Arctic (Osterman et al., 1999). Hanslik (PhD thesis, 2011) also documents an increase in agglutinated foraminifera (test cemented together from organic compounds, sand grains and other particles) further downcore. Following Seidenkrantz's (2013) observation, that there is a slight tendency of increasing sea-ice cover where calcareous foraminifera dominate, this increase in agglutinated specimens only further downcore also supports that the sea ice cover was more severe further up core where the calcareous *C. neoteretis* dominates. The occurrence of *C. reniforme*, a well-known indicator of cold glacio-marine paleoenvironments (Cronin et al., 2019), only in the upper 200 cm also presages ongoing climate cooling. Wollenburg and Mackensen (1998) mention that Arctic benthic foraminifera especially under permanent sea ice cover are usually smaller than at other ocean sites. Thus, the smaller test size of *C. neoteretis* compared to *C. teretis* could be an indicator for cooler conditions. It could however also have helped to be safe from predators. Guðmundsson et al. (2003) describe that scaphopods for example feed in quite specific size ranges and suggest that evolution has to some extent shaped the morphology of foraminifera to avoid predation. Only a small statistically significant decrease in test size from *C. teretis* to *C. neoteretis* was observed in this study, making it questionable if it is a reliable criterion to indicate a cooling climate.

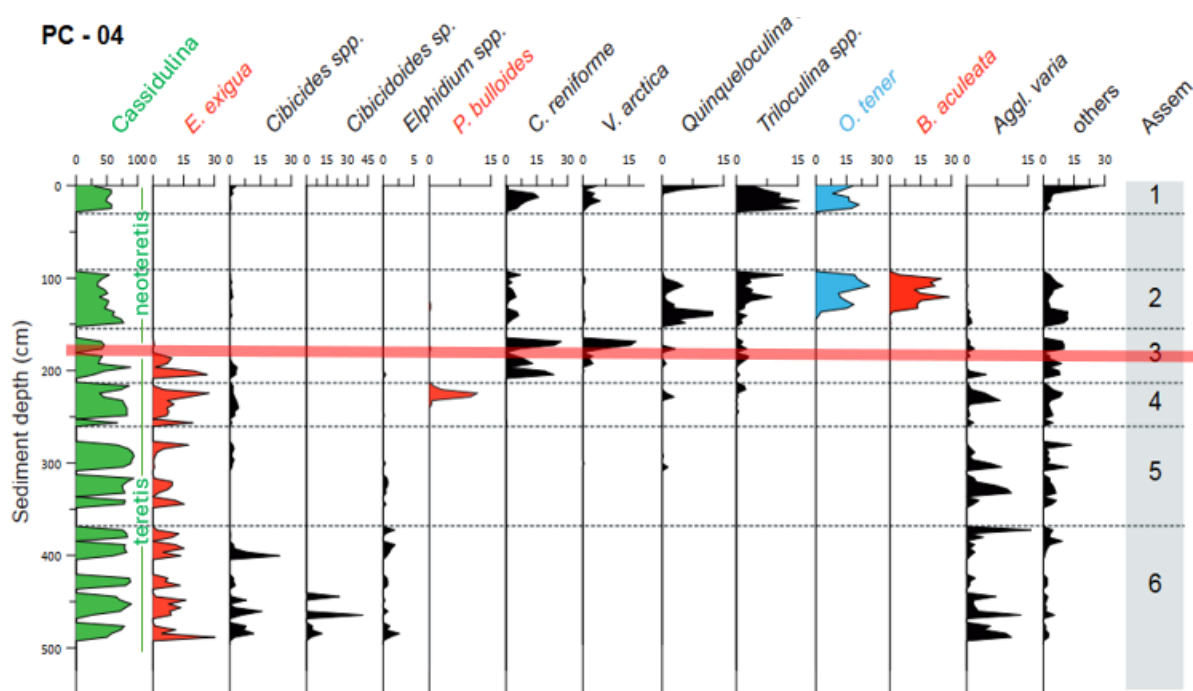


Fig. 15: Relative benthic foraminiferal abundance of the main species from core LOMROG07PC04. Modified from Hanslik (PhD thesis, 2011), Hanslik was not aware of the difference between *C. neoteretis* and *C. teretis*. The red line marks the transition depth between *C. neoteretis* and *C. teretis*.

Another support for a cooling climate comes from the beforementioned change in porosity. The oxygen-depleted conditions suggested by the larger pores could be caused by increasing sea ice

cover, blocking the gas exchange with the atmosphere, so that deep ocean waters eventually get depleted of oxygen from respiration (Cliff et al., 2021). In those oxygen-depleted conditions foraminifera with large pores would have an obvious evolutionary advantage. Water with higher salinity, as caused by formation of sea ice, can hold less oxygen than freshwater, further supporting the theory of an oxygen-depleted seafloor. Opposing this stands that colder water can in general hold more oxygen than warmer water, which would actually suggest higher oxygen levels in a colder climate.

Considering all that, the *C. neoteretis/teretis* transition could not only be used as an age marker, but also as an indicator for paleoclimatic conditions, possibly allowing assumptions on the extent of sea ice cover. Still, further research is necessary to assess this correlation. As Seidenkrantz (2013) mentions, benthic foraminifera are highly responsive to the food surplus often found at sea ice margins and might not actually be indicative of the sea ice cover itself. The reason of the extraordinary abundance of benthic foraminifera in LOMROG07PC04 compared to the only 100 km northeastern core LOMROG12PC03 might suggest that the sea ice margin ran there or that the sea ice cover occasionally broke open to allow the excessive amount of food expected for such a bloom of foraminifera. It could also be related to the water depth of the sites. According to Osterman et al. (1999), *C. neoteretis* is most common between 500 and 1100 m water depth and LOMROG07PC04 is located precisely within that range at 810 m water depth whereas LOMROG12PC03 is outside of the range at a water depth of 1607 m. A counterargument is brought by Wollenburg and Mackensen (1998), who found that the association of *C. teretis* is restricted to seasonally ice-free areas. As they researched living foraminifera, it is likely that they were referring to *C. neoteretis* instead of *C. teretis*. This would suggest that *C. neoteretis* can rather be associated with sea-ice margins or more moderate Arctic conditions than a full perennial sea ice cover. Overall, it is evident that *C. neoteretis* compared to *C. teretis* indicates climate cooling, but further research is necessary to determine the possible implications it could have on the extent of sea ice cover.

4.3 Meaning of apertural change

Another open question is the reason for the disappearance of teeth from *C. teretis* to *C. neoteretis*. A change in diet seems the most likely scenario for this morphological adjustment. To explore this possibility, changes in other benthic foraminifera records were examined. In the deep-sea benthic foraminifera record, a group of 95 species became extinct during the Mid-Pleistocene Transition (MPT)(Hayward et al., 2010). The MPT took place between 1,25 Ma and 0,7 Ma (Fig.16) and was characterized by an average increase in ice volume and a decrease in deep ocean temperatures (Clark et al., 2006). During the MPT, the times between interglacials changed from 40.000-year cycles (caused by the changes in obliquity of Earth) to 100.000-year cycles (caused by changes in the eccentricity of Earth's orbit), leading to more intense

glaciations. The beforementioned extinction event of the MPT was possibly a consequence of the decline or loss of their specific food source, as phytoplankton or prokaryotes would be more directly impacted by the cooling waters (Hayward et al., 2010). Hayward et al. (2010) mention that the extinction could be related to the function of their specialized apertures, a fate that might have also overtaken *C. teretis*. The teeth then might have been adapted to certain types of abundant phytodetritus, for example diatoms, which were not as readily available in the cooling climate. The evolutionary advanced *C. neoteretis* in that case would potentially rather feed from nanoplanktonic remains, bacteria, other food sources or potentially even just diatoms with different skeleton shapes. *C. neoteretis* is often associated with fine-grained, organic-rich mud (Seidenkrantz, 1995) which would allow it to feed on bacteria and organic matter from the sediment. In contrast to *C. neoteretis*, recent specimens of *C. laevigata* still have a serrated apertural flap with pronounced teeth. If the same logic is followed as before, this is not surprising, as *C. laevigata* lives in warmer environments than *C. neoteretis* and is dependent on a fresh phytodetritus supply (Alve, 2010).

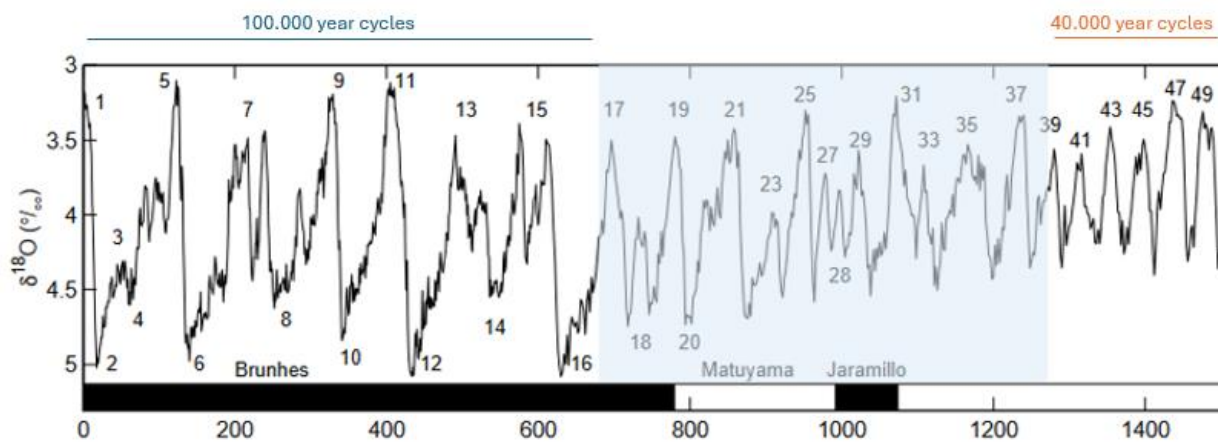


Fig. 16: Global benthic $\delta^{18}\text{O}$ records from the last 1,5 million years, indicating glacials (troughs) and interglacials (peaks). The x-axis reflects the age in Ka (1.000 years ago). The numbers along the graph show the Marine isotope stages (MIS). Marked in blue is the Mid-Pleistocene transition. Modified from Lisiecki and Raymo, 2005.

The two species *C.cf. reniforme* and *C. reniforme* could have a comparable history to *C. teretis* and *C. neoteretis*. They are similar in morphology, but it is possible to separate them by a few distinctive features. *C.cf. reniforme* has more pronounced teeth where *C. reniforme* only has remnants. That *C. reniforme* has not completely lost their teeth like *C. neoteretis* could suggest a broader food spectrum, or they could just be vestigial remains from evolution. *C.cf. reniforme* was found in older sediments stemming potentially from as far back as the Pliocene in the cores of IODP-EXP400, whereas *C. reniforme* is a still living benthic foraminifera. The first thereby could potentially be the ancestor of the latter. If there are more benthic foraminifera that lose their teeth with time this would clearly indicate a change in environmental conditions, for example a decrease, or change in seasonality or type, of phytoplankton, that caused this evolutionary development. Too little information is known about *C.cf. reniforme* to make any confident conclusions in this direction, but it is a promising new direction of research that could deliver another piece in the puzzle of the Arctic past.

4.4 Age models and tentative dating of the *C. neoteretis/teretis* transition

Most age models in the Arctic have been revised multiple times over the last decades and many have been proven wrong. It was therefore chosen to provide all results in this study exclusively based on sediment depth, so that a certain age can be assigned to them when more valid age models for the Arctic exist. Nevertheless, I have experimented with an age model as a crude test to explore the existing constraints and gain potentially useful new information from *Cassidulina*. In this context, I put a number on the *C. neoteretis/teretis* transition by using a recent age model based on nannofossils which exists for core LOMROG12PC03. In the age model of Razmjooei et al. (2023), the last appearance of the nannofossil *Pseudoemiliania lacunosa* is assigned an age of around 0,48 Ma (million years ago). In core LOMROG12PC03 the last appearance of *P. lacunosa* happens at 125 cm depth, loosely coinciding with the *C. neoteretis/teretis* transition (Fig.17). Based on this, the *C. neoteretis/teretis* transition at the Southern Lomonosov Ridge can be estimated to have happened approximately half a million years ago.

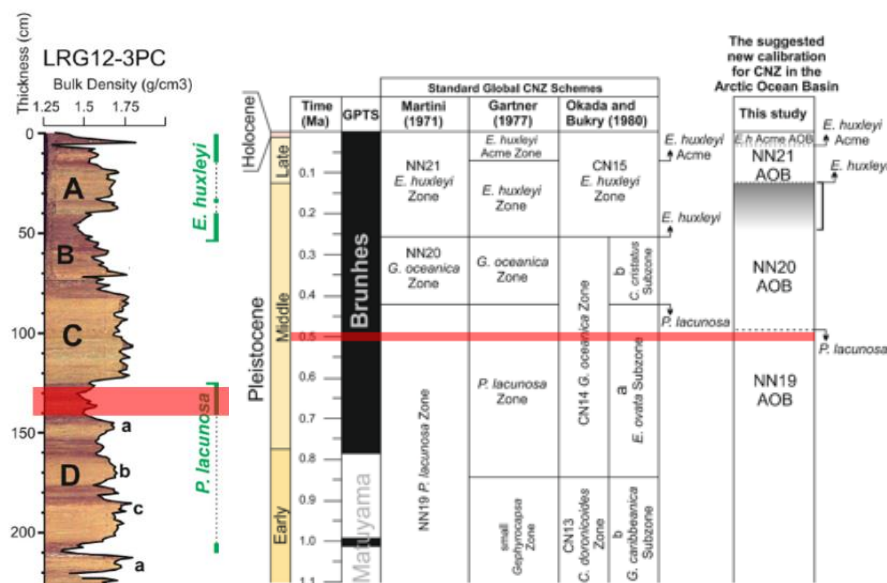


Fig. 17: Stratigraphy of core LOMROG12PC03 with nannofossil age markers and newly suggested adjustments on existing age models. Marked in red is the *C. neoteretis/teretis* transition. Modified from Razmjooei et al. (2023).

If Seidenkrantz's (1995) assumptions are correct and *C. neoteretis* evolved 2,3-2,0 Ma ago and migrated northward to the Norwegian Sea by 0,7 Ma, it is not unreasonable to assume it arrived at the Lomonosov Ridge 0,2 million years later. It needs to be further explored why and when *C. teretis* went extinct. If it really went extinct later in the Arctic than in the North Atlantic, that might suggest that *C. teretis* was in fact outcompeted and replaced by its better adapted descendant *C. neoteretis* as it migrated. That the *C. neoteretis/teretis* transition occurs at a slightly deeper depth in LOMROG07PC04 (approx. 40 cm deeper than at LOMROG12PC03) could in that case be a sign of an earlier arrival of *C. neoteretis* connected to the more Southern location. The depth

difference could however also be caused by higher sedimentation rates at LOMROG07PC04, such that the *C. neoteretis/teretis* transition is time equivalent in LOMROG12PC03. Considering that LOMROG07PC04 might have been located at the sea ice margin, is closer to the Greenland shelf and the distance between both sites is only 100 km, a higher sedimentation rate is the more valid possibility. This is further supported by O'Regan et al. (2019), who describe LOMROG12PC03 as more compressed (lower sedimentation rate) than other cores from the Lomonosov Ridge. If it is confirmed by more research that the *C. neoteretis/teretis* transition happened at the same time in this region, it could be used to correlate lithological units of different cores.

The reason Lazar et al. (2016) did not find the clear transition in the Western Arctic and found predominantly smooth apertural features only in the most recent sediments (in the uppermost 10 cm) could in that case be owed to a relatively recent arrival of *C. neoteretis* in the Western Arctic. Moreover, the age model used by Lazar et al. (2016) is probably outdated by now and not considering the most recent perspectives by Razmjooei et al (2023), leaving their temporal placement unsubstantiated. *C. neoteretis* is known to be an indicator for intermediate Atlantic Water (Cage et al., 2021), which circulates anticlockwise around the Arctic (Fig.5), thereby possibly being the migration channel for *C. neoteretis*. The Atlantic Ocean has a higher salinity and a pole-to-pole overturning circulation with deep-water formation in the North Atlantic, which the Pacific Ocean is missing (Ferreira et al., 2018), providing very different living conditions for benthic foraminifera. However, the surface water circulation is also crucially important for benthic foraminifera, as the surface production determines their food supply, one of the most important factors in benthic foraminiferal growth. The late arrival of *C. neoteretis* in the Western Arctic and the absence in core AO16-8GC could be explained by the stronger influence of Pacific Water and freshwater from the Beaufort Gyre, whereas the other cores researched in this study where *C. neoteretis/C. teretis* was found were all receiving more direct influx of Atlantic Water (Fig.5). Tracing *C. neoteretis/teretis* throughout the Arctic could therefore also help with the understanding of ocean currents. Wollenburg and Mackensen (1998) bring forward that availability of food and competition are the predominant controls on benthic foraminiferal associations and bottom current activities, water mass and sediment type are of minor importance, so caution has to be taken with such interpretations.

Lazar and Polyak (2016) describe a similar turnover in foraminiferal assemblages in core P23 in the Western Arctic as the one witnessed by Hanslik (PhD thesis, 2011) in core LOMROG07PC04. From an abundance of *E. exigua* there is a shift towards polar-type foraminifera like *Stetsonia horvathi*. They assign this turnover to the end of the MPT (see Fig.16). Also here, unfortunately, the age models that Lazar and Polyak (2016) were applying have since been revised and the ages they assigned are probably much too young, making their interpretations questionable. According to Seidenkrantz (1995) the last occurrence of *C. teretis* in the Norwegian Sea was below the Brunhes-Matuyama boundary, around 0,7 Ma. This would align with the end of the MPT and could be the reason for a newly empowered campaign of *C. neoteretis*. If the

estimations of this study are correct, the transition from *C. teretis* to *C. neoteretis* happened later at the Lomonosov Ridge, around 0,5 Ma, within Marine Isotope Stage (MIS) 13. This could be the time delay that *C. neoteretis* needed to migrate northward, in this case the transition there could be a delayed reaction to the end of the MPT. As *C. neoteretis* already evolved between 2,0 and 2,3 Ma, the replacement of *C. teretis* by *C. neoteretis* could also just have been a slow process continuously proceeding since the intensification of the Northern Hemisphere Glaciation 2,7 Ma (Hayashi et al., 2020).

As long as there is no coherent age model for Quaternary Arctic Ocean sediments, all this remains highly speculative. Further research on sedimentation rates and a reconciliation of existing regional age models is necessary to come to confident conclusions.

4.5 Evaluation of the utility

Cronin et al. stated in 2019 that it is not practical to break chambers off specimens and that the variability is too great to use apertural structures for species-level taxonomy. In this study it was found that breaking chambers off was indeed not practical, but also rarely necessary for species identification. Even though the variability is acknowledged here (see chapter 3.3, Morphological variability), and it is sometimes not possible to identify an individual specimen by looking at the aperture morphology, it was possible for each sample depth to distinguish between *C. neoteretis* and *C. teretis* by observing the range of apertural features in several specimens. The existence of one serrated apertural flap within a multitude of smooth ones can be regarded as the exception that proves the rule. This is in line with Cage et al. (2021) who observed that usually only one of the two species is present, and it is enough to investigate the best-preserved specimens to determine which one it is. But well-preserved specimens are not always readily available - in this study the state of preservation was the major limitation. Even a sample bustling with foraminifera could prove to be useless, if it was mostly recrystallized or agglutinated fragments that do not reveal the key features. Especially the aperture was very susceptible to fracturing and was even in well-preserved specimens often damaged, which complicates identification (Plate 14,1). Recrystallization was common in different horizons of all researched cores and made the classification of a smooth or serrated apertural flap exceedingly difficult (Plate 14,2). Apertures that looked smooth on first sight in some cases turned out to be just broken off (Plate 14,3). In fact, only 32 % of the apertures in LOMROG07PC04 were undamaged. In the worst-case scenario, not even identification of the genus was possible (Plate 14,4). In the cores IODP-EXP400-U1606B and U1608A the low amount of poorly preserved specimens allowed few confident interpretations. It must be admitted that the utility of the *C. neoteretis/C.teretis* transition is limited to sites that contain a minimal number of well-preserved specimens.

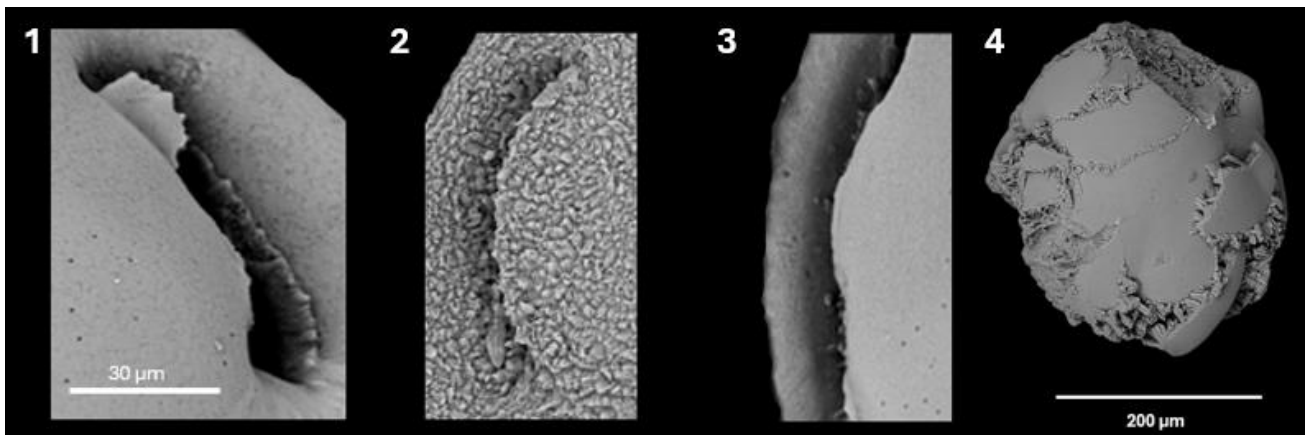


Plate 14: 1-3: Specimens from core LOMROG07PC04 that show how poor preservation can affect the morphology of the aperture. 4: Poorly preserved and fractured specimen with neomorphic crystal growth from core IODP-EXP400-U1608A. Scale bar from 1 applies to 2 and 3 as well.

A valid point made by Lazar et al. (2016) is that a scanning electron microscope is necessary to see the serration of the apertural flap, which is not always readily available. The light microscope images can already give a general idea by the size of the specimens, the nature of the keel and umbilical boss. Sometimes, in especially well-preserved large specimens, the teeth are even already visible. For a definitive judgement, SEM images are indeed necessary. However, all SEM images in this study are taken with a relatively simple desktop SEM that is also being used on research vessels. With careful preselection of samples under the light microscope and validation from selected specimens through SEM images, the differentiation between *C. neoteretis* and *C. teretis* is certainly possible, even on Arctic expeditions. Even though the work can be time consuming and requires a high level of precision and detail, in a world of scarce information the bestowed effort could be of big value.

4.6 Critical Reflection

The selection of foraminifera in this study could potentially be biased towards smaller specimens, as larger ones were more often damaged; or towards larger specimen as smaller ones are more readily overlooked. Moreover, the distribution by density caused by the sprinkling of the sample could have affected the results, possibly leading to a size bias in certain areas of the sampling tray. Especially for the morphological measurements this could make a difference. The issue could be avoided in a future project by using a microsampler, which reduces the samples to a more evenly manageable size. Also, as the tests are not completely flat, it was oftentimes not possible to get an image of the whole umbilical side from straight above, so the leaning of the specimen could have obscured the measurements and influenced the appearance on images. The same applies to the pore size where it was not always possible to find a spot where the pores could be seen from straight above and may appear smaller or more elongated because of that. However, since the methods were consistently followed, the same bias should apply to all results, making them, if not precise, at least comparable. The not normal

distribution of test diameters in the morphometrical samples could indicate a too small sample size, it is however more likely to be caused by the existence of several extremely large outliers positively skewing the distribution, which is not unreasonable in nature. As the spearman correlation was used, this should not affect the statistical results.

Most data could only be collected from well-preserved specimens, which are mostly not readily available throughout the sedimental record, causing potentially important changes in times of bad preservation to be overseen. A large percentage of specimens are quite challenging to interpretate, as broken apertures or crystallized textures blurring distinctive features complicate the identification. The interpretation of the data could therefore be biased by subjective perceptions. All SEM images that were used for major interpretations in this study are added in the appendix, making it possible for readers to come to their own conclusions (Appendix A).

4.7 Future research opportunities

This study has shown that a variety of questions remain unanswered, but that there is exciting potential in the research of *Cassidulina*. If the *C. neoteretis/teretis* transition would be tracked in more regions of the Arctic Ocean, it could tell us a story not only about the evolution and migration of these species but possibly about changes in paleoclimate and sea ice cover. More confident age models are necessary to accurately find a time for the transition, but if this time is set for various regions, the transition could be used as a regional biostratigraphic age marker. Due to the connection of *C. neoteretis* to intermediate Atlantic water, gaining more information on the spreading of *C. neoteretis* throughout the Arctic also allows conclusions on the ocean currents that were prevailing at the time. Investigations on living specimen of *C. neoteretis* could also be helpful in understanding their morphology and ecology and help to make conclusions about the past. In a world of global warming, it would also be interesting to monitor how *C. neoteretis* will react on the continuously less severe sea ice cover of the Arctic Ocean.

Another exciting prospect could be the investigated research in *C.cf reniforme* that has not yet been properly analysed and described. One could exploit the possibility if it could be the ancestor to *C. reniforme*. In this context it would also be interesting to see if the disappearance of teeth is a regular occurrence in benthic foraminifera and if it temporally aligns even between different species. It would be a great test of this hypothesis to research if the diet of *C. laevigata*, that still has a clearly serrated aperture with teeth, has not changed over time.

Conclusion

This study answered the question if *C. neoteretis* can reliably be distinguished from *C. teretis* based on morphological features. It can, under the premise that the abundance of foraminifera and the state of preservation is adequate, by comparing the most prominent differences under the SEM: a smooth apertural flap in *C. neoteretis* and distinctively larger pores compared to the teeth and smaller pores of *C. teretis*. The slightly smaller test and umbilical boss size as well as the more prominent flattened peripheral keel of *C. neoteretis* can aid the identification under the light microscope. A confident taxonomic placement can only be made considering all different key characteristics of several well-preserved specimen.

The *C. neoteretis/C. teretis* transition was found at two core sites at the Southern Lomonosov Ridge at sediment depths between 127 cm and 183 cm, which were due to the most recent age model dated within MIS13. If it is confirmed in more areas with more data and more reliable age models, the transition has great potential to be a biostratigraphic age marker as well as an indicator for a cooling climate and the extent of Arctic sea ice cover.

Acknowledgements

Special thanks goes to my supervisor Helen Coxall, who made this exciting project possible and always had helpful advice and enthusiasm. Further gratitude shall be bestowed on Marit-Solveig Seidenkrantz and Anne Jennings for their outstanding expertise and support, Kjell Jansson for guidance with the SEM, Tirza Weitkamp and Flor Vermassen for helping with the practical challenges of foraminifera research, and Samuel Lundström and Marie Gehres for their unconditional love and encouragement.

References

- Ald, S.M., Leander, B.S., Simpson, A.G.B., Archibald, J.M., Anderson, R., Bass, D., Bowser, S.S., Brugerolle, G.B., Farmer, M.A., Karpov, S., Kolisko, M., Lane, C.E., Logde, D.J., Mann, D.G., Meisterfeld, R., Mendoza, L., Moestrup, O., Mozley-Standridge, S.E., Smirnov, A.V., Spiegel, F., 2007. Diversity, Nomenclature, and Taxonomy of Protists., *Systematic Biology*, 56 (4) , 684–689.
- Alexanderson, H., Backman, J., Cronin, T. M., Funder, S., Ingólfsson, Ó., Jakobsson, M., Landvik, J. Y., Löwemark, L., Mangerud, J., März, C., Möller, P., O'Regan, M., Spielhagen, R. F., 2014. An Arctic perspective on dating Mid-Late Pleistocene environmental history, *Quaternary Science Reviews*, 92, 9-31.

- Alve, E.**, 2010. Benthic foraminiferal responses to absence of fresh phytodetritus: A two-year experiment. *Marine Micropaleontology*, 76 (3–4), 67-75.
- Armstrong, H. A., Brasier, M. D.**, 2005. *Microfossils*, 2nd Edition. Blackwell, Oxford.
- Backman, J., Jakobsson, M., Lovlie, R., Polyak, L., Febo, L.A.**, 2004. Is the central Arctic Ocean a sediment starved basin? *Quaternary Science Reviews*, 23, 1435-1454.
- Boudagher-Fadel, M.K.**, 2008. Evolution and Geological Significance of Larger Benthic Foraminifera. *Developments in Palaeontology and Stratigraphy*, 21.
- Bulian, F., Kouwenhoven, T.J., Andersen, N., Krijgsman, W., Sierro, F.J.**, 2022. Reflooding and repopulation of the Mediterranean Sea after the Messinian Salinity Crisis: Benthic foraminifera assemblages and stable isotopes of Spanish basins. *Marine Micropaleontology*, 176, 1-29.
- Burke, J. E., Renema, W., Henehan, M. J., Elder, L. E., Davis, C. V., Maas, A. E., Foster, G. L., Schiebel, R., Hull, P. M.**, 2018. Factors influencing test porosity in planktonic foraminifera, *Biogeosciences*, 15, 6607–6619.
- Cage, A.G., Pienkowski, A., Jennings, A., Knudsen K.L., Seidenkrantz, M.S.**, 2021. Comparative analysis of six common foraminiferal species of the genera *Cassidulina*, *Paracassidulina*, and *Islandiella* from the Arctic–North Atlantic domain. *Journal of Micropalaeontology*, 40, 37–60.
- Clark, P.U., Archer, D., Pollard, D., Blum, J.D. Rial, J.A., Brovkin, V., Mix, A.C., Pisias, N.G., Roy, M.**, 2006. The middle Pleistocene transition: characteristics, mechanisms, and implications for long-term changes in atmospheric pCO₂. *Quaternary Science Reviews*, 25 (23–24), 3150-3184.
- Cliff, E., Khatiwala, S., Schmittner, A.**, 2021. Glacial deep ocean deoxygenation driven by biologically mediated air–sea disequilibrium. *Nature Geoscience*, 14, 43–50.
- Cronin, T.M., Seidenstein, J., Keller, K., McDougall, K., Ruefer, A., Gemery, L.**, 2019. The Benthic Foraminifera *Cassidulina* from The Arctic Ocean: Application to Palaeoceanography and Biostratigraphy. *Micropaleontology*, 65, 105–125.
- du Châtelet, E., Francescangeli, F., Bouchet, V.M.P., Frontalini, F.**, 2018. Benthic foraminifera in transitional environments in the English Channel and the southern North Sea: A proxy for regional-scale environmental and paleo-environmental characterisations. *Marine Environmental Research*, 137, 37-48.
- Dumitriu, S., Dubicka, Z., Ionesi, V.**, 2018. The functional significance of the spinose keel structure of benthic foraminifera: Inferences from *Miliolina cristata* Millett, 1898 (*Miliolida*) from northeast Romania. *Journal of Micropalaeontology*, 37, 153-166.

- Farmer, J.R., Cronin, T.M., Thunell, R.C., Keigwin, L.D., Willard, D.,** 2010. Holocene Climate Variability in the Beaufort Sea, Arctic Ocean from Benthic Foraminifers, Stable Isotopes and Pollen. AGU Fall Meeting Abstracts.
- Ferreira, D., Cessi, P., Coxall, H.K., De Boer, A., Dijkstra, H.A., Drijfhout, S.S., Eldevik, T., Harnik, N., McManus, J.F., Marshall, D.P., Nilsson, J., Roquet, F., Schneider, T., Wills, R.C.,** 2018. Atlantic-Pacific Asymmetry in Deep Water Formation. *Annual Review of Earth and Planetary Sciences*, 46, 327–352.
- Galeotti, S. & Coccioni, R.,** 2001. Morphometric Analysis of Selected Benthic Foraminifera from Cape Roberts Project (CRP) and CIROS-1 Cores, Victoria Land Basin, Antarctica. *Terra Antarctica*, 8 (4), 359-368.
- Giraldo-Gomez, V. M., Petrizzo, M.R., Erba, E., Bottini, C.,** 2022. Biostratigraphy, paleobathymetry and paleobiogeography of Lower Cretaceous benthic foraminifera from Shatsky Rise (ODP Leg 198) in the central Pacific Ocean. *Cretaceous Research*, 138, 1-23.
- Gooday, A.J. & Jorissen, F.J.,** 2012. Benthic Foraminiferal Biogeography: Controls on Global Distribution Patterns in Deep-Water Settings. *Annual Review of Marine Sciences*, 4, 237-262.
- Guðmundsson, G., Engelstad, K., Steiner, G., Svavarsson, J.,** 2003. Diets of four deep-water scaphopod species (Mollusca) in the North Atlantic and Nordic Seas. *Marine Biology*, 142, 1103-1112.
- Hanslik, D.,** 2011. Late Quaternary Biostratigraphy and Palaeoceanography of the central Arctic Ocean. Meddelanden från Stockholms Universitets Institution för Geologiska Vetenskaper, 345.
- Hayashi, T., Yamanaka, T., Hikasa, Y., Sato, M., Kuwahara, Y., Ohno, M.,** 2020. Latest Pliocene Northern Hemisphere glaciation amplified by intensified Atlantic meridional overturning circulation. *Communications Earth & Environment*, 1, 25.
- Haynes, J.R.,** 1981. Foraminifera. Palgrave MacMillan, London.
- Hayward, B.W., Johnson, K., Sabaa, A.T., Kawagata, S., Thomas, E.,** 2010. Cenozoic record of elongate, cylindrical, deep-sea benthic foraminifera in the North Atlantic and equatorial Pacific Oceans. *Marine Micropaleontology*, 74 (3-4), 75-95.
- Jakobsson, M., Løvlie, R., Al-Hanbali, H., Arnold, E., Backman, J., Mörth, M.,** 2000. Manganese and color cycles in Arctic Ocean sediments constrain Pleistocene chronology. *Geology*, 28 (1), 23–26.
- Jakobsson, M., Marcussen C., LOMROG Scientific Party,** 2008. Lomonosov Ridge off Greenland 2007 (LOMROG) - Cruise Report, 122 pp. *Special Publication Geological Survey of Denmark and Greenland*, Copenhagen, Denmark.
- Lazar, K.B. & Polyak, L.,** 2016. Pleistocene benthic foraminifers in the Arctic Ocean: Implications for sea-ice and circulation history. *Marine Micropaleontology*, 126, 19-30.

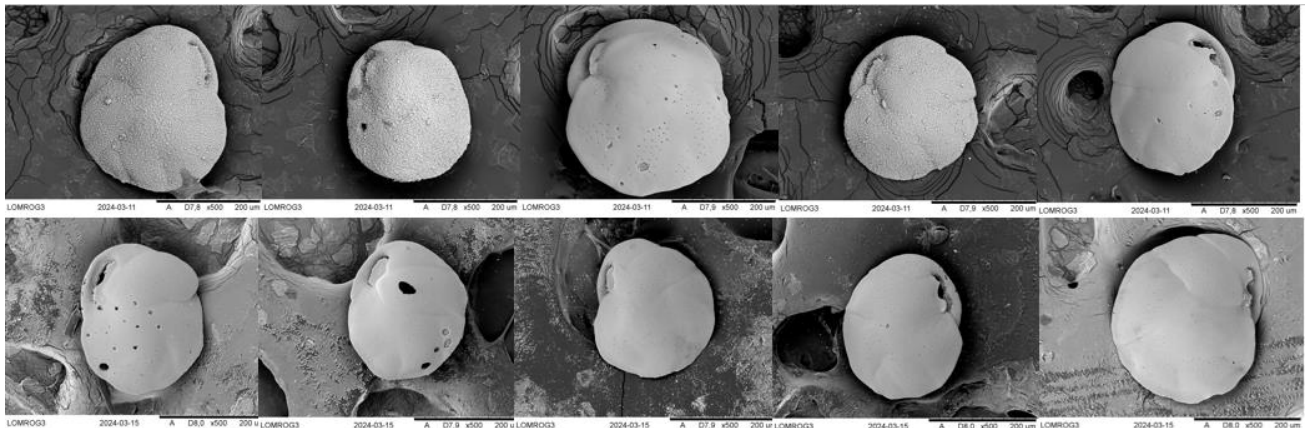
- Lazar, K.B., Polyak, L., Dipre, G.R.,** 2016. Re-examination of the use of *Cassidulina neoteretis* as a Pleistocene biostratigraphic marker in the Arctic Ocean. *Journal of Foraminiferal Research*, 46 (2), 115-123.
- Lisiecki, L.E. & Raymo, M.E.,** 2005. A Pliocene-Pleistocene stack of 57 globally distributed benthic $\delta^{18}O$ records. *Paleoceanography*, 20, 1003.
- Loeblich, A.R., Tappan, H.,** 1988. Foraminiferal Genera and Their Classification. Springer, New York.
- Majewski, W., Szczuciński, W., Gooday, A.J.,** 2023. Unique benthic foraminiferal communities (stained) in diverse environments of sub-Antarctic fjords, South Georgia, *Biogeosciences*, 20, 523-544.
- Murray, J.,** 2006. Ecology and Applications of Benthic Foraminifera. Cambridge: Cambridge University Press.
- O'Regan, M., Coxall H.K., Cronin, T.M., Gyllencreutz, R., Jakobsson, M., Kaboth, S., Löwemark, L., Wiers, S., West, G.,** 2019. Stratigraphic Occurrences of Sub-Polar Planktic Foraminifera in Pleistocene Sediments on the Lomonosov Ridge, Arctic Ocean. *Frontiers in Earth Science*, 7.
- O'Regan, M., King, J. Backman, J., Jakobsson, M., Pälike, H., Moran, K., Heil, C., Sakamoto, T., Cronin T.M., Jordan, R.W.,** 2008. Constraints on the Pleistocene chronology of sediments from the Lomonosov Ridge. *Paleoceanography*, 23, PA1S19.
- Osterman, L.E.,** 1996. Pliocene and Quaternary benthic foraminifera from Site 910, Yermak Plateau. *Proceedings of the Ocean Drilling Program, Scientific Results*, 151, 187–195.
- Osterman, L.E., Poore, R.Z., Foley, K.M.,** 1999. Distribution of benthic foraminifera (>125 μ m) in the surface sediments of the Arctic Ocean. *United States Geological Survey Bulletin*, 2164, 28.
- Patterson, R.T., McKillop, W.B., Kroker, S., Nielsen, E., Reinhardt, E.G.,** 1997. Evidence for rapid avian-mediated foraminiferal colonization of Lake Winnipegosis, Manitoba, during the Holocene Hypsithermal. *Journal of Paleolimnology*, 18, 131-143.
- Petersen, J., Riedel, B., Barras, C., Pays, O., Guihéneuf, A., Mabilieu, G., Schweizer, M., Meysman, F.J.R., Jorissen, F.J.,** 2016. Improved methodology for measuring pore patterns in the benthic foraminiferal genus *Ammonia*. *Marine Micropaleontology*, 128, 1-13.
- Rasband, W.S.,** 1997-2018. ImageJ, U. S. National Institutes of Health, Bethesda, Maryland, USA, <https://imagej.net/ij/>.
- Razmjooei, M.J., Henderiks, J., Coxall, H.K., Baumann, K., Vermassen, F., Jakobsson, M., Niessen, F., O'Regan, M.,** 2023. Revision of the Quaternary calcareous nannofossil biochronology of Arctic Ocean sediments, *Quaternary Science Reviews*, 321, 108382.

- Santana, B.F.B.B., Freitas, T.R., Leonel, J., Bonetti, C.,** 2021. Biometric and biomass analysis of Quaternary Uvigerinidae (Foraminifera) from the Southern Brazilian continental slope. *Marine Micropaleontology*, 169, 102041.
- Schönfeld, J., Alve, E., Geslin, E., Jorissen, F.J., Korsun, S., Spezzaferri, S.,** 2012. The FOBIMO (FORaminiferal Blo-MONitoring) initiative—Towards a standardised protocol for soft-bottom benthic foraminiferal monitoring studies. *Marine Micropaleontology*, 94–95, 1-13.
- Sejrup, H. P., & Guilbault, J. P.,** 1980. *Cassidulina reniforme* and *C. obtusa* (Foraminifera), taxonomy, distribution, and ecology. *Sarsia*, 65(2), 79–85.
- Seidenkrantz, M.S.,** 1995. *Cassidulina teretis* Tappan and *Cassidulina neoteretis* new species (Foraminifera): stratigraphic markers for deep sea and outer shelf areas. *Journal of Micropaleontology*, 14, 145-157.
- Seidenkrantz, M.S.,** 2013. Benthic foraminifera as palaeo sea-ice indicators in the subarctic realm – examples from the Labrador Sea–Baffin Bay region, *Quaternary Science Reviews*, 79, 135-144.
- Tappan, H.,** 1951. Northern Alaska index Foraminifera. *Contributions from the Cushman Foundation for Foraminiferal Research*, 2, 1-8.
- Tremblay, B., Newton, R., Cullather, R.,** 2005. An Ice Free Arctic?. AGU Fall Meeting Abstracts.
- Wang, F., Yang S., Zhai B., Gong S., Wang J., Fu X., Yi J., Ning, Z,** 2023. Pore density of the benthic foraminiferal test responded to the hypoxia off the Changjiang estuary in the East China Sea. *Frontiers in Marine Science*, 10.
- Wollenburg, J.E., Mackensen, A.,** 1998. Living benthic foraminifera from the central Arctic Ocean: faunal composition, standing stock and diversity. *Marine Micropaleontology*, 34 (3–4), 153-185.

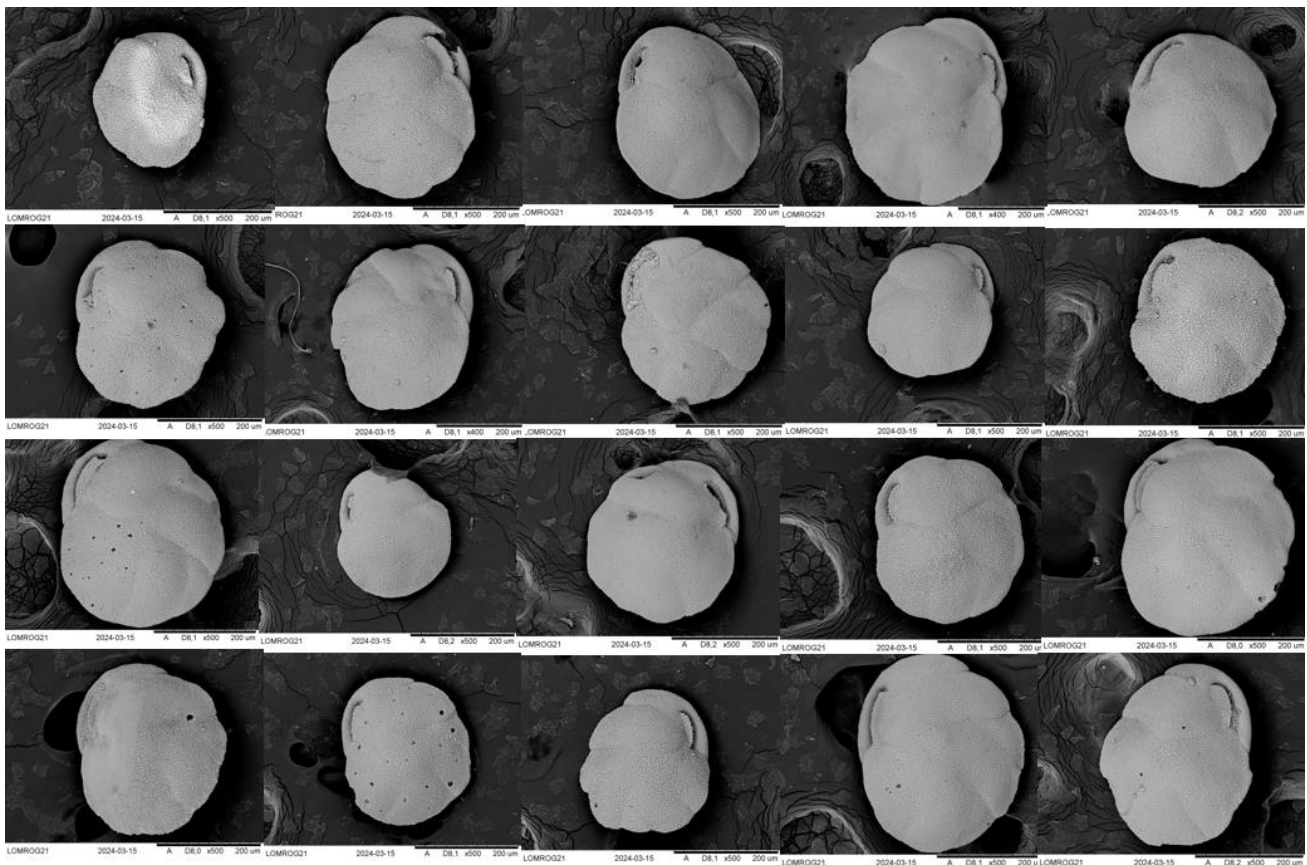
Appendix A SEM images

LOMROG07PC04

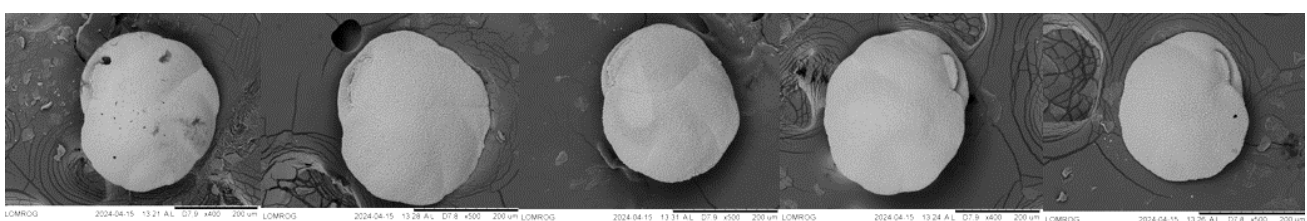
2-3 cm



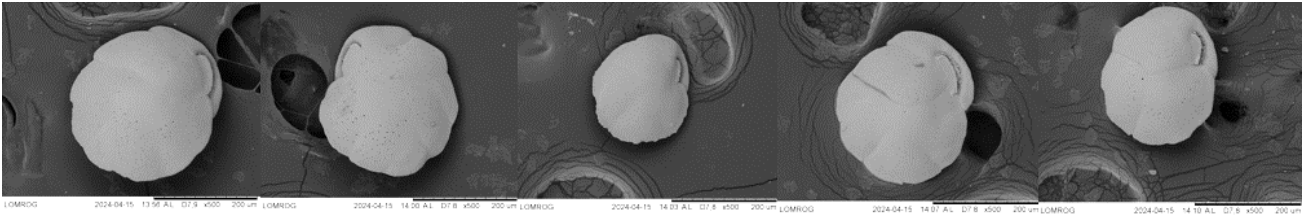
20-21 cm



98-99 cm



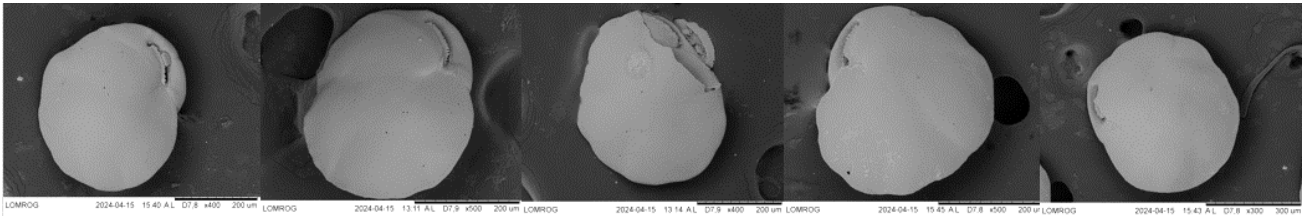
166-167 cm



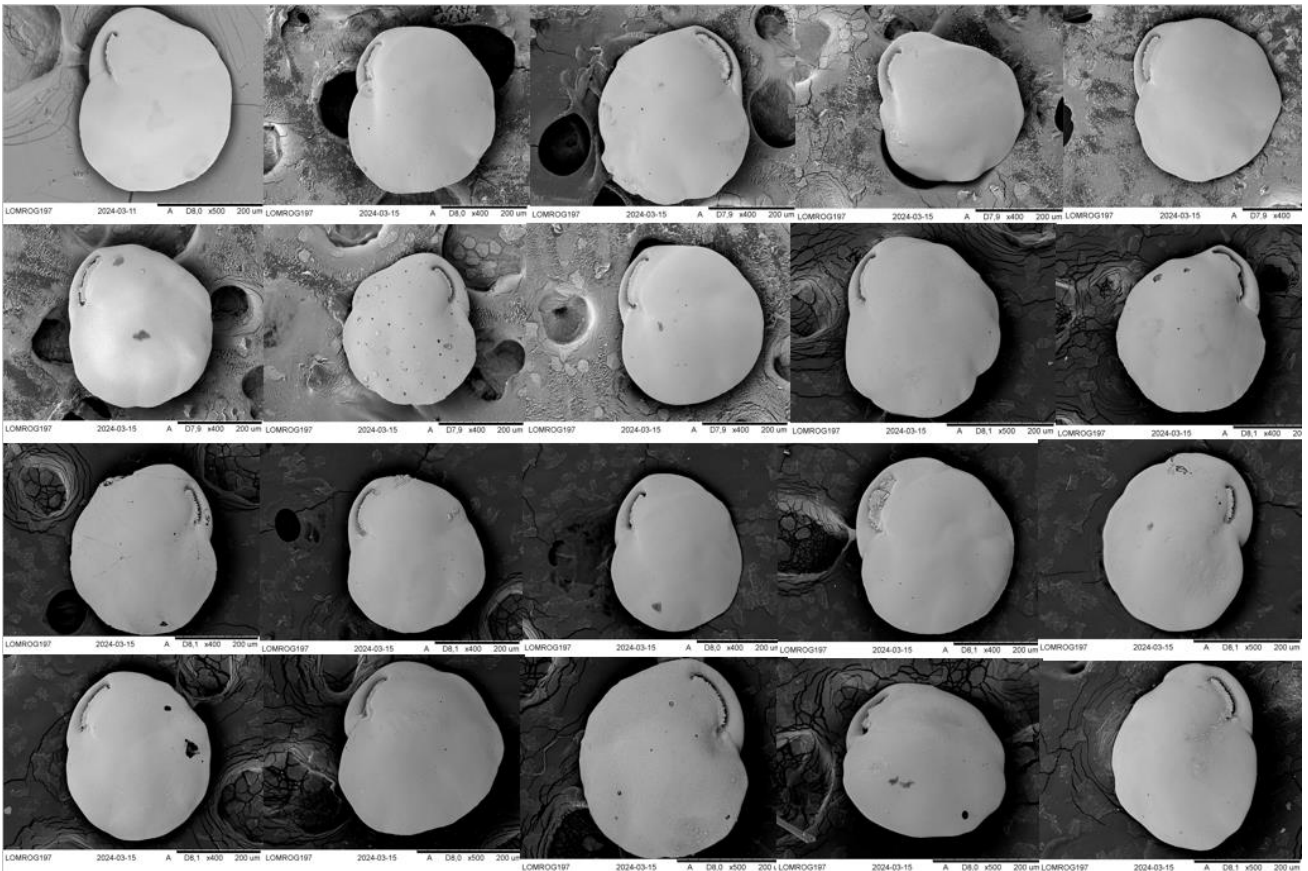
170-171 cm



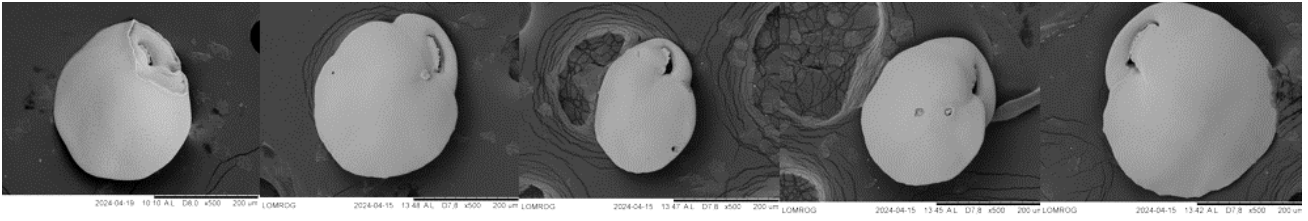
182-183 cm



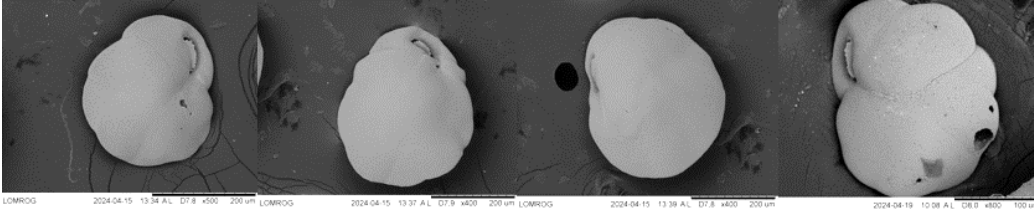
196-197 cm



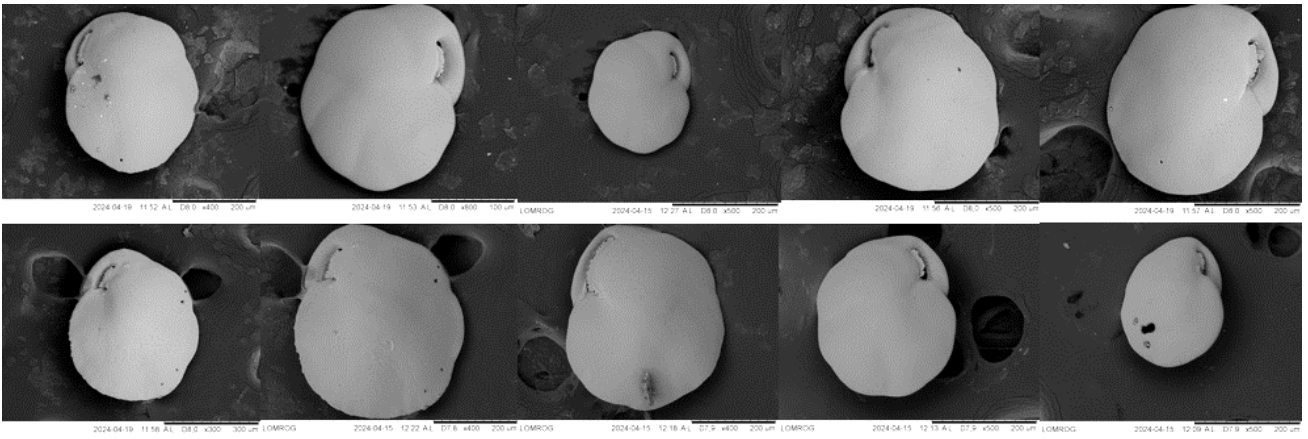
330-331 cm



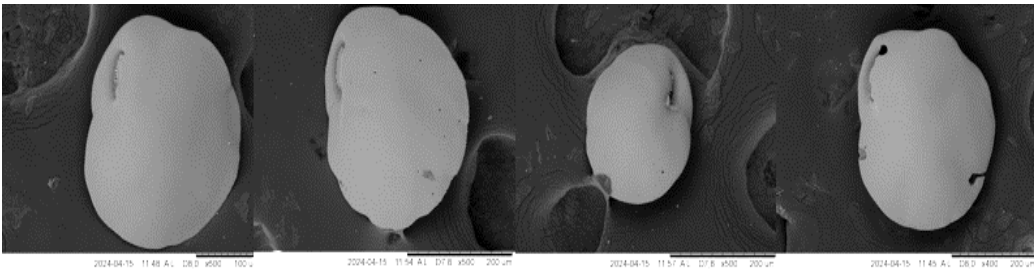
374-375 cm



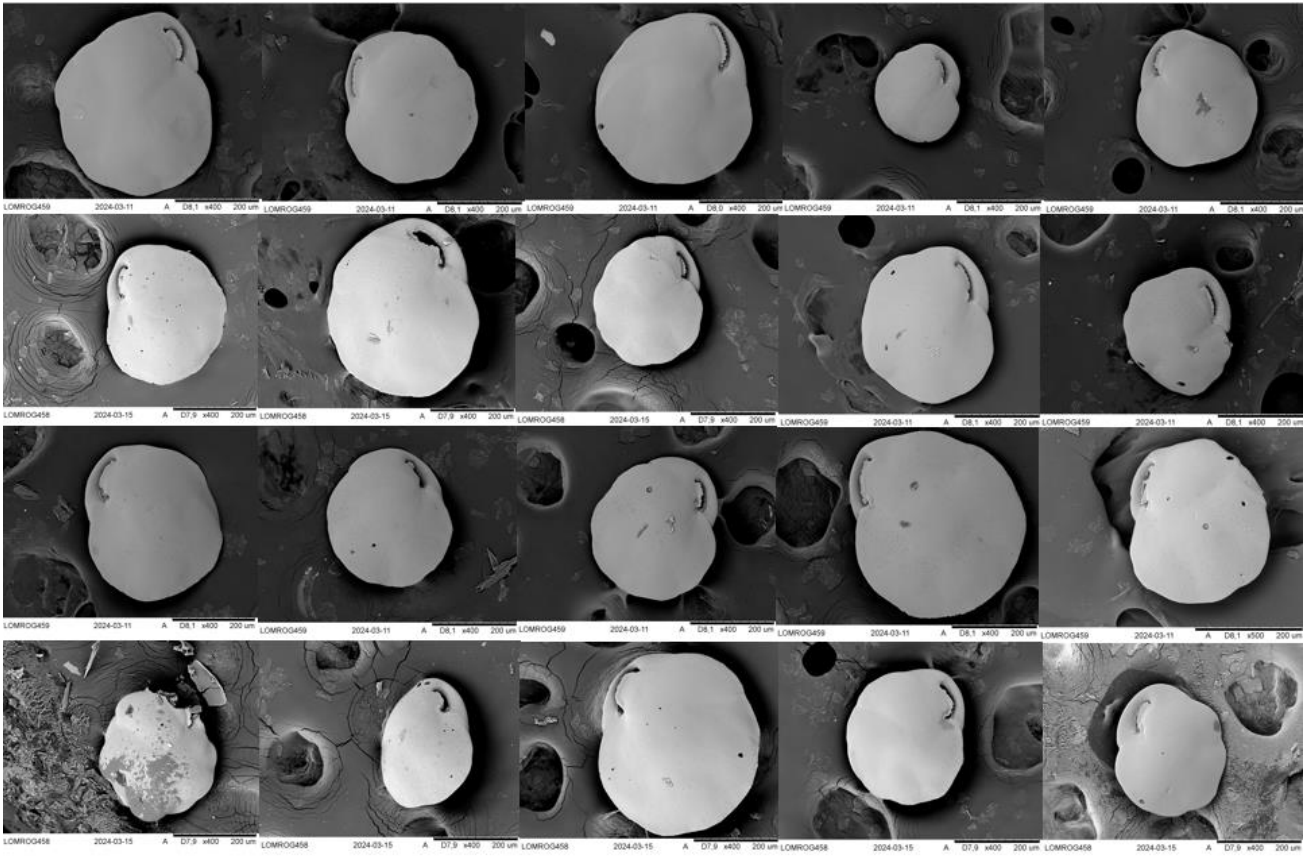
398-399 cm



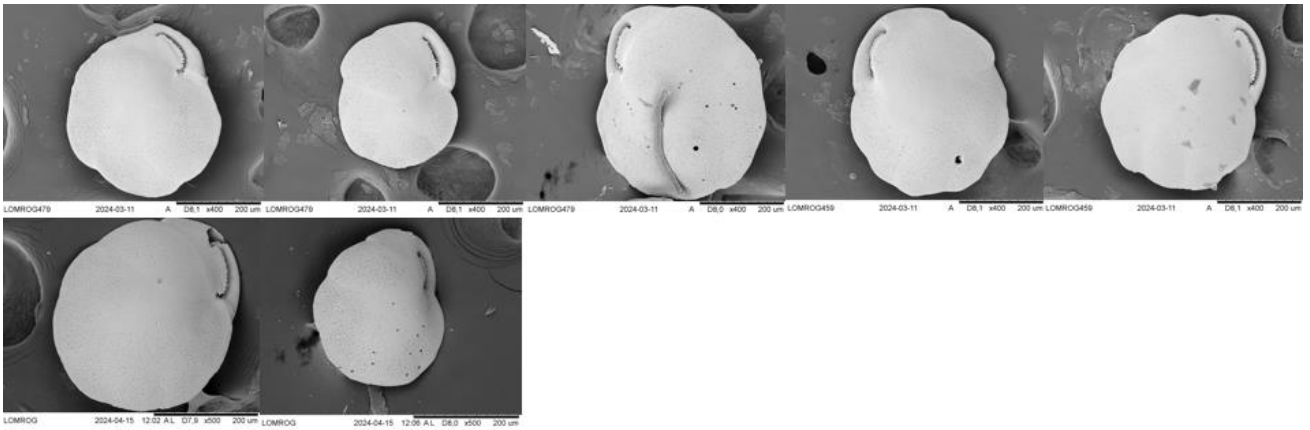
430-431 cm



458-459 cm

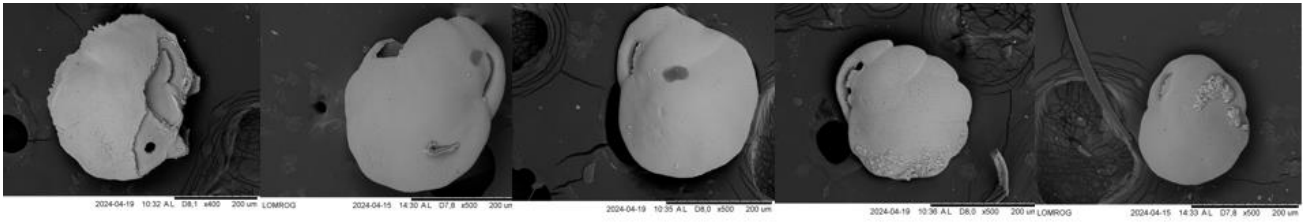


478-479 cm



LOMROG12PC03

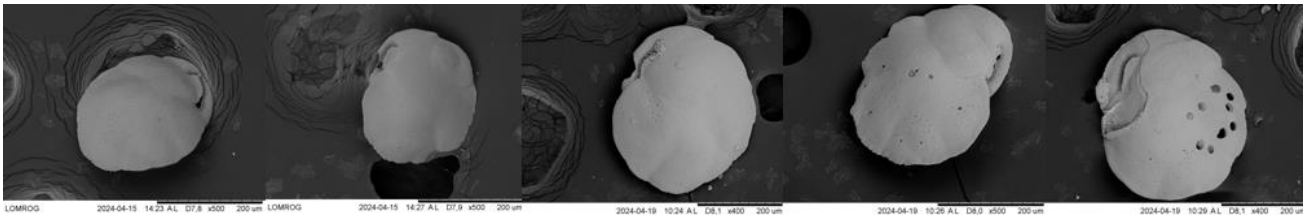
42 cm



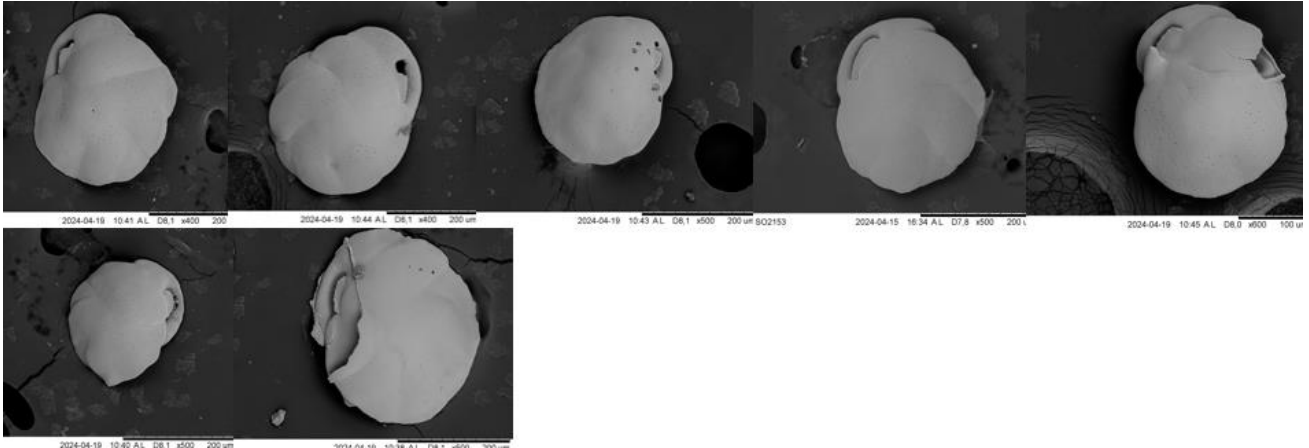
74 cm



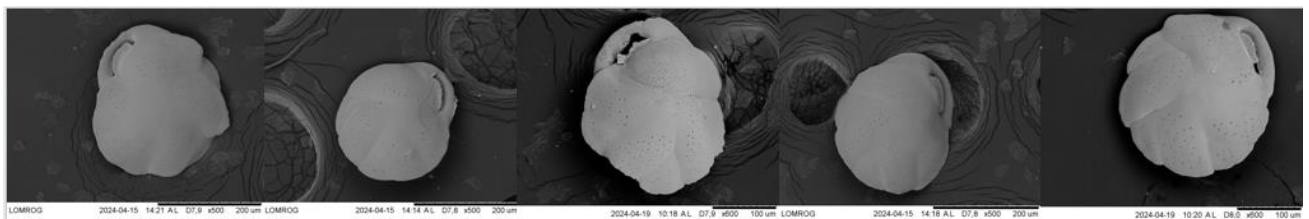
76 cm



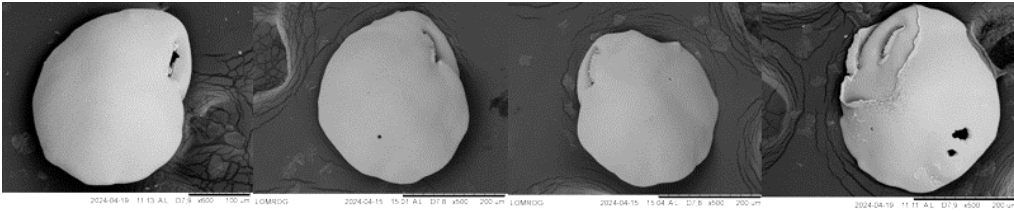
82 cm



127 cm



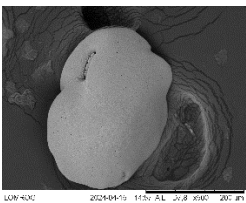
142 cm



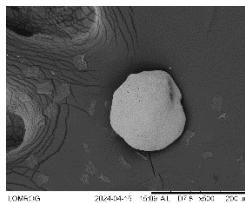
157 cm



172 cm



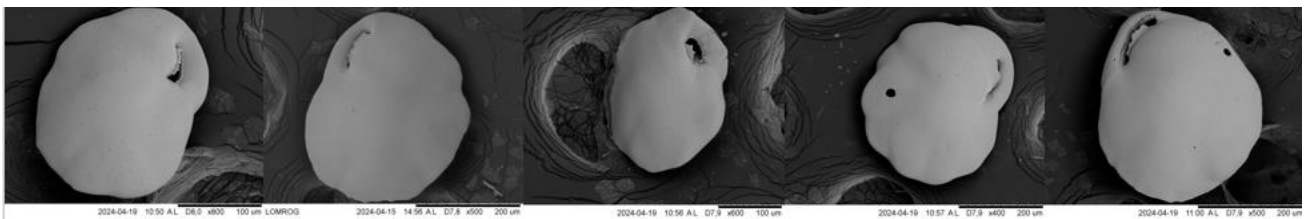
184 cm



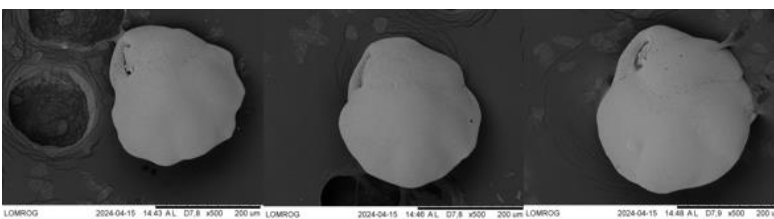
207 cm



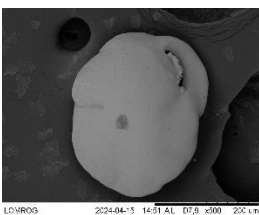
211 cm



219 cm



352 cm



Light microscope images of all specimens and close-up SEMs from apertures are available on request.

Appendix B data tables

1	2	3	4	5
0,52	0,323	0,456	0,433	0,491
0,584	0,584	0,329	0,788	0,504
0,777	0,491	0,433	0,584	0,323
0,413	0,387	0,713	0,433	0,387
0,551	0,551	0,532	0,584	0,392
0,721	0,433	0,595	0,581	0,52
0,329	0,376	0,504	0,329	0,645
0,392	0,504	0,387	0,595	0,547
0,329	0,456	0,456	0,258	0,635
0,491	0,532	0,258	0,465	0,581
0,5107	0,4637	0,4663	0,505	0,5025

Appendix B1: Pore diameters of five different specimens of *C. obtuse* from Core 93030-03IBC at 6-7 cm depth.

1	2	3	4	5
0,654	0,731	0,836	0,731	0,669
0,39	0,843	1,136	0,748	0,731
0,654	0,953	0,836	0,803	0,548
0,75	0,654	0,78	0,58	0,69
0,58	0,717	0,58	0,717	0,705
0,644	0,772	0,918	0,918	0,405
0,467	0,862	0,833	0,731	0,513
0,821	0,772	0,327	0,836	0,467
0,769	0,855	0,793	0,962	0,453
0,641	0,907	0,717	0,9	0,577

Appendix B2: Pore diameters of five different specimens of *C. reniforme* from Core 2008029-59PC at 303-305 cm depth.

1	2	3	4	5
1,239	1,143	0,785	0,849	1,161
0,983	1,163	1,233	1,761	1,034
1,050	1,654	1,034	0,903	0,520
1,797	1,034	0,976	1,582	0,849
1,582	1,355	0,968	1,613	0,939
1,177	0,861	0,710	1,649	0,983
1,618	1,042	1,002	1,548	1,114
1,925	1,163	0,841	1,419	1,002
1,443	0,899	1,114	1,361	1,163
1,099	1,064	0,710	1,233	0,899

Appendix B3: Pore diameters of five different specimens of *C.cf. reniforme* from Core IODP EXP400-U1606B-14R-CC.

1	2	3	4	5
2.124	1.410	1.541	1.220	1.805
2.088	1.307	1.583	1.501	1.975
2.087	1.571	1.726	1.259	1.872
2.051	1.524	1.623	1.462	1.836
2.131	1.476	1.814	1.290	1.623
1.726	1.233	1.524	1.544	1.863
1.703	1.419	1.376	0.933	1.962
1.664	1.272	1.384	1.156	1.540
1.732	1.245	1.296	1.423	1.348
1.805	1.453	1.410	1.245	1.245
1.911	1.391	1.528	1.344	1.707

Appendix B4: Pore diameters of five different specimens of *C. laevigata* from Core 93030-03IBC at 6-7 cm depth.

1	2	3	4	5
1,149	1,306	1,104	0,841	1,032
1,369	0,713	1,050	0,664	0,924
1,127	0,866	1,127	0,970	1,316
0,816	1,095	1,050	1,200	1,050
1,342	0,917	1,099	0,736	1,161
1,425	0,710	1,040	0,648	1,226
1,104	0,839	1,227	1,010	0,849
1,104	1,081	1,034	1,415	1,190
1,104	1,020	1,040	0,939	1,097
1,356	0,987	1,285	1,110	1,305

Appendix B5: Pore diameters of five different specimens of *C. neoteretis* from Core 200802959PC at 303-305 cm depth.

1	2	3	4	5
0,785	0,452	0,71	0,635	0,71
0,547	0,433	0,456	0,516	0,635
0,635	0,289	0,408	0,609	0,595
0,645	0,347	0,347	0,465	0,532
0,52	0,266	0,323	0,52	0,456
0,456	0,387	0,465	0,52	0,504
0,347	0,413	0,387	0,452	0,452
0,47	0,266	0,577	0,52	0,452
0,452	0,376	0,698	0,491	0,329
0,456	0,323	0,686	0,584	0,658

Appendix B6: Pore diameters of five different specimens of *C. teretis* from Core LOMROG07PC04 at 300-301 cm depth.

smooth aperture	undetermined	serrated aperture	depth
5	5	0	3 cm
9	11	0	21 cm
2	12	0	107 cm
6	10	1	146 cm
4	1	0	167 cm
2	3	0	171 cm
0	3	3	183 cm
0	8	12	197 cm
0	8	6	243 cm
0	5	15	301 cm
0	1	10	399 cm
0	9	11	459 cm
0	1	6	479 cm

Appendix B7: Number of specimens of *C. neoteretis/teretis* through Core LOMROG07PC04 categorized by the shape of their apertural flap.

depth in cm	maximum length in μm	minimum length in μm	average length in μm	STD	SEM
3	371,1	222,9	285,159	35,3	12,632
21	413,26	226,51	304,833	41,33	14,79
99	388,232	152,33	273,881	51,262	18,344
107	380,74	227,76	289,491	42,12	15,073
127	417,813	165,557	277,000	72,452	25,927
147	456,79	212,06	331,778	67,373	24,109
171	482,51	195,709	302,116	77,195	27,625
197	422,92	308,44	364,324	27,599	9,877
223	490,528	189,289	301,813	60,98	21,823
243	582,7	280,73	376,590	71,117	25,45
287	512,344	185,129	306,250	77,853	27,86
301	445,08	200,02	271,191	50,229	17,975
331	487,416	149,398	293,629	90,963	32,552
375	521,584	200,892	329,210	61,4	21,973
399	446,104	161,963	276,002	79,737	28,535
431	447,805	166,703	286,450	64,805	23,191
455	559,05	222,97	393,520	105,203	37,648
479	663,806	214,335	358,339	104,559	37,417

Appendix B8: Morphological measurements of test diameters of *Cassidulina neoteretis/teretis* at different depths in Core LOMROG07PC04 with standard deviation (STD) and standard error of the mean (SEM). Full data table of all individual measurements available on request.

2-3 cm					114-115 cm				
1	2	3	4	5	1	2	3	4	5
0,877	0,774	0,721	0,695	0,826	0,658	0,555	0,924	0,959	0,906
0,695	1,233	0,861	0,849	0,408	0,635	0,612	0,584	1,042	1,168
0,721	0,906	0,47	0,752	0,785	0,698	0,52	0,866	0,939	0,816
0,808	0,896	0,52	0,868	0,452	0,777	0,516	0,785	0,839	1,042
0,581	0,816	0,392	0,516	0,713	0,755	0,551	0,877	1,008	0,551
0,674	0,839	0,555	0,581	0,609	0,78	0,695	0,648	0,987	0,777
0,968	0,849	0,635	0,658	0,609	0,695	0,532	0,71	1,002	1,064
1,074	0,968	0,774	0,788	0,645	0,551	0,465	0,983	0,664	0,924
0,93	0,785	0,658	0,736	0,584	0,912	0,456	0,584		0,976
0,841	0,777	0,612	0,491	0,595	0,551	0,465	0,987		0,774
146-147 cm					166-167 cm				
1	2	3	4	5	1	2	3	4	5
0,906	0,635	1,042	0,577	0,826	0,798	0,912	0,584	0,648	0,736
0,939	0,721	1,184	0,635	0,877	0,877	1,297	0,755	0,713	0,721
0,839	1,02	0,785	0,713	1,127	0,877	0,839	0,609	0,721	0,97
0,785	0,976	0,906	0,584	0,877	1,04	1,385	0,595	0,785	1,032
0,97	0,755	1,143	0,635	0,821	1,184	0,664	0,736	0,736	1,042
0,987	0,721	0,785	0,577	0,777	0,577	0,52	0,866	0,658	0,774
0,903	0,78	0,97	0,664	0,785	0,595	0,798	0,664	0,695	0,516
0,645	0,777	0,808	0,376	0,577	0,713	1,533	0,635	0,584	0,721
0,839	0,939	0,736	0,516	0,721	0,452	0,71	0,648	0,491	1,268
0,849		0,612	0,645	0,584	0,912	1,01	0,939	0,78	0,581
182-183 cm					196-197 cm				
1	2	3	4	5	1	2	3	4	5
0,841	0,52	0,595	0,645	0,584	0,645	0,491	0,839	0,581	0,516
0,47	0,47	0,664	0,452	0,755	0,551	0,581	0,903	0,452	0,612
0,577	0,581	0,532	0,658	0,433	0,808	0,52	0,658	0,452	0,695
0,584	0,47	0,266	0,258	0,584	0,581	0,329	0,721	0,577	0,52
0,433	0,465	0,323	0,452	0,408	0,635	0,456	0,826	0,387	0,645
0,555	0,595	0,648	0,376	0,329	0,635	0,323	0,71	0,387	0,674
0,376	0,532	0,755	0,612	0,52	0,721	0,347	0,609	0,52	0,465
0,551	0,595	0,595	0,491	0,266	0,532	0,347	0,47	0,258	0,491
0,392	0,433	0,551	0,555	0,365	0,713	0,266	0,777	0,452	0,774
0,551	0,581	0,52	0,387	0,581	0,645	0,392	0,674	0,452	0,551
300-301 cm					398-399 cm				
1	2	3	4	5	1	2	3	4	5
0,785	0,452	0,71	0,635	0,71	0,516	0,555	0,695	0,516	0,648
0,547	0,433	0,456	0,516	0,635	0,323	0,413	0,736	0,595	0,645
0,635	0,289	0,408	0,609	0,595	0,392	0,71	0,648	0,584	0,658
0,645	0,347	0,347	0,465	0,532	0,491	0,612	0,664	0,721	0,347
0,52	0,266	0,323	0,52	0,456	0,595	0,903	0,52	0,721	0,433
0,456	0,387	0,465	0,52	0,504	0,233	0,52	0,555	0,456	0,516
0,347	0,413	0,387	0,452	0,452	0,433	0,721	0,648	0,648	0,516
0,47	0,266	0,577	0,52	0,452	0,323	0,721	0,648	0,695	0,329

0,452	0,376	0,698	0,491	0,329	0,52	0,839	0,52	0,721	0,532
0,456	0,323	0,686	0,584	0,658	0,648	0,877	0,392	0,71	0,329
430-431 cm					458-459 cm				
1	2	3	4	1	2	3	4	5	
0,581	0,577	0,408	0,504	0,289	0,323	0,387	0,551	0,645	
0,648	0,595	0,456	0,648	0,433	0,47	0,347	0,555	0,504	
0,516	0,584	0,387	0,645	0,392	0,465	0,376	0,456	0,52	
0,258	0,452	0,635	0,516	0,547	0,323	0,233	0,465	0,456	
0,52	0,555	0,233	0,516	0,547	0,376	0,376	0,365	0,877	
0,456	0,504	0,323	0,584	0,635	0,408	0,233	0,639	0,52	
0,52	0,408	0,456	0,392	0,323	0,323	0,266	0,551	0,645	
0,347	0,47	0,785	0,433	0,204	0,465	0,347	0,866	0,645	
0,52	0,635	0,387	0,329	0,408	0,504	0,266	0,504	0,52	
0,595	0,547	0,274	0,584	0,347	0,387	0,289	0,452	0,664	

Appendix B9: Pore diameters of *Cassidulina neoteretis/teretis* at different depths in Core LOMROG07PC04.

depth in cm	mean pore size in μm	STD	SEM
3	0,727	0,171	0,047
115	0,773	0,192	0,053
147	0,793	0,171	0,048
167	0,798	0,234	0,065
183	0,515	0,126	0,035
197	0,563	0,154	0,043
300	0,491	0,126	0,035
399	0,574	0,151	0,042
431	0,495	0,121	0,034
459	0,454	0,148	0,041

Appendix B10: Mean pore size diameters of *Cassidulina neoteretis/teretis* at different depths in Core LOMROG07PC04 with standard deviation (STD) and standard error of the mean (SEM).

depth in cm	% sinistral	% dextral
3	60	40
21	63	37
99	73	27
107	55	45
127	65	35
147	50	50
170	43	57
197	67	33
223	50	50
243	48	52
287	47	53
301	50	50
331	65	35
375	57	43
399	50	50
431	53	47
455	50	50
479	53	47

Appendix B11: Percentages of coiling direction of *C. neoteretis/teretis* at different depths in Core LOMROG07PC04.